ISSN 8755-6839

SCIENCE OF **TSUNAMI HAZARDS**

Journal of Tsunami Society International

Volume 30 **Number 3** **2011**

WWW.TSUNAMISOCIETY.ORG

TSUNAMI SOCIETY INTERNATIONAL, 1741 Ala Moana Blvd. #70, Honolulu, HI 96815, USA.

SCIENCE OF TSUNAMI HAZARDS is a CERTIFIED OPEN ACCESS Journal included in the prestigious international academic journal database DOAJ, maintained by the University of Lund in Sweden with the support of the European Union. SCIENCE OF TSUNAMI HAZARDS is also preserved, archived and disseminated by the National Library, The Hague, NETHERLANDS, the Library of Congress, Washington D.C., USA, the Electronic Library of Los Alamos, National Laboratory, New Mexico, USA, the EBSCO Publishing databases and ELSEVIER Publishing in Amsterdam. The vast dissemination gives the journal additional global exposure and readership in 90% of the academic institutions worldwide, including nation-wide access to databases in more than 70 countries.

OBJECTIVE: Tsunami Society International publishes this interdisciplinary journal to increase and disseminate knowledge about tsunamis and their hazards.

DISCLAIMER: Although the articles in SCIENCE OF TSUNAMI HAZARDS have been technically reviewed by peers, Tsunami Society International is not responsible for the veracity of any statement, opinion or consequences.

Submit manuscripts of research papers, notes or letters to the Editor. If a research paper is accepted for publication the author(s) must submit a scan-ready manuscript, a Doc, TeX or a PDF file in the journal format. Issues of the journal are published electronically in PDF format. There is a minimal publication fee for authors who are members of Tsunami Society International for three years and slightly higher for non-members. Tsunami Society International members are notified by e-mail when a new issue is available. Permission to use figures, tables and brief excerpts from this journal in scientific and educational works is granted provided that the source is acknowledged.

Recent and all past journal issues are available at: http://www.TsunamiSociety.org CD-ROMs of past volumes may be purchased by contacting Tsunami Society International at postmaster@tsunamisociety.org Issues of the journal from 1982 thru 2005 are also available in PDF format at the Los Alamos National Laboratory Library http://epubs.lanl.gov/tsunami/

ISSN 8755-6839

SCIENCE OF **TSUNAMI HAZARDS**

Journal of Tsunami Society International

Volume 30 **Number 3** **2011**

THE RESPONSE OF MONTEREY BAY TO THE GREAT TOHOKU EARTHQUAKE OF 2011

L. C. Breaker[1], T. S. Murty[2], D. Carroll[1] and W. J. Teague[3]

[1] Moss Landing Marine Laboratories, Moss Landing, CA 93950
[2] University of Ottawa, Ottawa, Canada
[3] Naval Research Laboratory, Stennis Space Center, MS 39529

ABSTRACT

The response of Monterey Bay to the Great Tohoku earthquake of 2011 is examined in this study. From a practical standpoint, although the resulting tsunami did not cause any damage to the open harbors at Monterey and Moss Landing, it caused extensive damage to boats and infrastructure in Santa Cruz Harbor, which is closed to surrounding waters. From a scientific standpoint, the observed and predicted amplitudes of the tsunami at 1 km from the source were 21.3 and 22.5 m based on the primary arrival from one DART bottom pressure recorder located 986 km ENE of the epicenter. The predicted and observed travel times for the tsunami to reach Monterey Bay agreed within 3%. The predicted and observed periods of the tsunami-generated wave before it entered the bay yielded periods that approached 2 hours. Once the tsunami entered Monterey Bay it was transformed into a seiche with a primary period of 36-37 minutes, corresponding to quarter-wave resonance within the bay. Finally, from a predictive standpoint, major tsunamis that enter the bay from the northwest, as in the present case, are the ones most likely to cause damage to Santa Cruz harbor.

Keywords: *Great Tohoku earthquake, Monterey Bay, damage reports, singular spectrum analysis, seiche modes*

1. INTRODUCTION

On March 11, 2011 at 05:46 UTC, one of the five largest earthquakes since 1900 hit the coast of Japan. It has been called The Great Tohoku Earthquake and had a magnitude (M_W) of 9.0, according to the Japanese Meteorological Agency (JMA) and the U.S. Geological Survey (USGS). It occurred 373 km northeast of Tokyo. The Pacific Tsunami Warning Center issued a tsunami warning for the entire Pacific Ocean within 2 hours after the earthquake occurred. Along the coasts of California and Oregon, tsunami-generated surges of up to 2.4 m hit some areas, causing major damage to docks and harbors. At Crescent City, California, the tsunami produced a wave height of 7 feet (2.1 m), a location where extensive damage occurred. A state of emergency was declared for several counties in California including Del Norte, Humboldt, San Mateo, and Santa Cruz.

Monterey Bay is directly exposed to the open ocean with an entrance that is almost as wide as the bay itself. It has three harbors, one at Monterey at the south end of the bay, a second at Moss Landing at the center of the bay, and a third at Santa Cruz at the north end of the bay (Fig. 1). Between 8:00AM and 9:00AM PDT, sudden increases in water level of almost a meter were reported at Monterey and Moss Landing. The Pacific Tsunami Warning Center (PTWC) reported a peak amplitude in water level of 70 cm at Monterey (B. Shiro, personal communication). No significant damage to infrastructure or boating was reported at either location. However, at Santa Cruz Harbor extensive damage did occur. Conservative estimates indicate that losses to infrastructure in Santa Cruz Harbor approach $30M and that up to 100 boats experienced significant damage resulting in losses that exceed $5M. Unlike Monterey and Moss Landing, the Santa Cruz Harbor is essentially closed and so was unable to accommodate the incoming waters associated with the tsunami leading to amplified surges and the resulting damage.

2. MATERIALS AND METHODS

a. Sources of Data

The data used in this report come from three sources. First, bottom pressure data were acquired from the Monterey Accelerated Research System (MARS) array (www.mbari.org/MARS/). The array is located beyond the entrance of Monterey Bay on a ridge near the edge of Monterey Submarine Canyon at a depth of 891m, approximately 25 km west-northwest of Monterey (Fig. 1). The pressure data from the MARS array was converted to equivalent sea surface height via the hydrostatic equation. Second, water levels at one-minute resolution were acquired from the tide gauge in Monterey Harbor. This tide gauge is part of NOAA's National Water Level Observation Network (NWLON) operated and maintained by the National Ocean Service. Finally, bathymetric data from the U.S. Navy with 2-minute resolution along a great circle path from the tsunami's point of origin to the MARS array was used to calculate expected travel times (Ko, 2009).

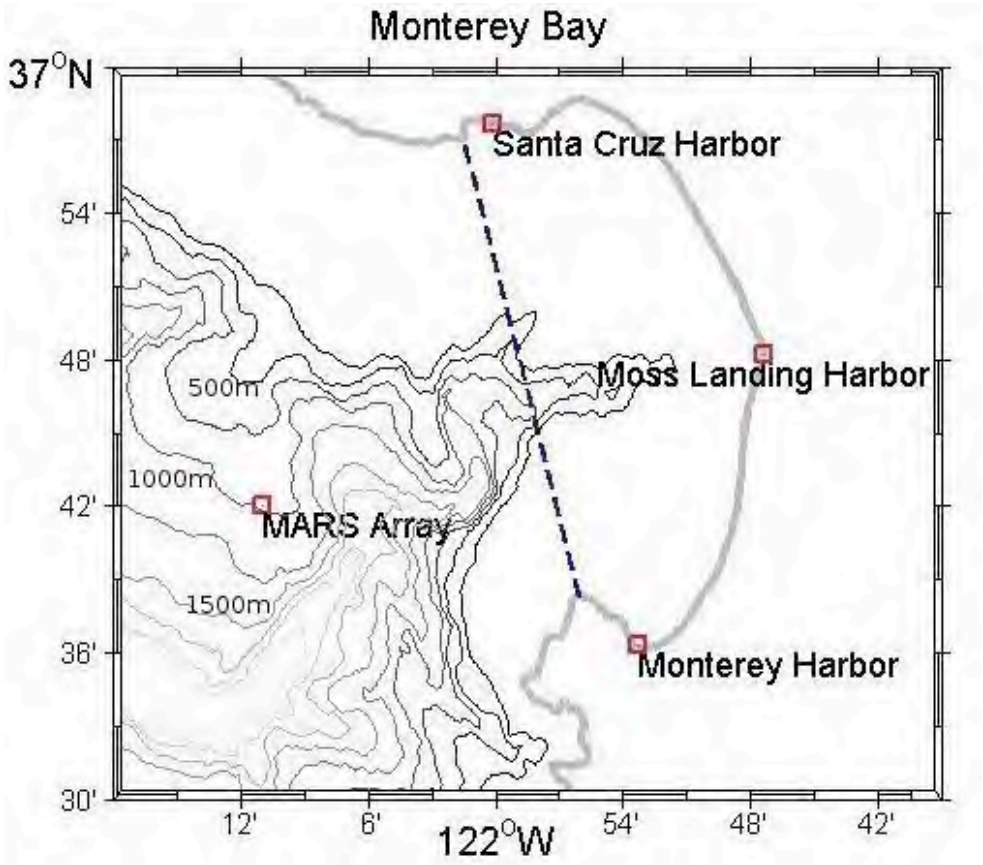

Fig. 1. This figure shows Monterey Bay together with the location of the MARS array where the pressure data were acquired, and the three harbors within the bay. The dashed line represents the expected nodal location for the transverse mode of oscillation for Monterey Bay.

b. Method of Analysis

To examine the response of Monterey Bay, Singular Spectrum Analysis (SSA) was employed (e.g., Breaker et al., 2011). SSA is a method of decomposing a time sequence into a set of independent modes, similar in many respects to Principal Component Analysis (PCA). Because of the adaptive nature of the basis functions employed the method is well-suited for analyzing records that are nonstationary and/or nonlinear (e.g., Vautard et al., 1992). SSA can be applied to short, noise-like time series, making it well-suited for use in this study.

A lagged covariance matrix is formed from the time sequence (a Toeplitz matrix in this case) that is decomposed into eigenvalues, eigenvectors and principal components. Reconstructed components can be calculated from the eigenvectors and principal components that represent partial time series whose sum over all modes reproduces the original time series. The number of modes that are selected is called the window length and determines the resolution of the decomposition. The results of the SSA analysis are presented in the following section.

3. RESULTS

a. Initial Conditions

The epicenter of the Great Tohoku Earthquake was located approximately 72 km east of the Oshika Peninsula of Tōhoku at a depth of 32 km. This event has been categorized as an undersea megathrust rupture that occurred along the Japan Trench subduction zone with the Pacific Plate subducting beneath the plate that underlies northern Honshu. The rupture caused the sea floor to rise by 5 - 8 meters. According to the JMA, the earthquake may have ruptured the fault zone over a length of 500 km and a width approaching 200 km. The JMA analysis also indicated that the earthquake itself was comprised of a set of three events. The co-seismic, vertical motion of the seafloor produced a devastating tsunami that was felt over the entire Pacific basin. Tectonically generated vertical subsidence likely intensified the tsunami. The Tohoku earthquake was followed by three aftershocks that exceeded 7.0 M_w within 45 minutes of the main event.

We have extracted the arrival sequences for the Great Tohoku Earthquake from three Deep-ocean Assessment and Reporting of Tsunamis (DART) bottom pressure recorders (www.ndbc.noaa.gov/dart/dart.shtml). DART bottom pressure recorders 21418, 21401, and 21413 were employed. The DART recorders are located in deep water away from coastal influences at distances of 551, 986, and 1224 km, East, ENE and SE of the epicenter. We have estimated the amplitude of the tsunami at 1 km from the source assuming cylindrical spreading and thus the effects of refraction have not been taken into account. The primary signals were distinct at 21413 and 21401 but not at 21418 and so we have not included the results from this location.

To obtain a first-guess value for the amplitude we have used the following empirical relation: $Log_{10}H = 0.75 \cdot M_w - 5.07$, where H is the amplitude in meters and M_w is the earthquake magnitude (Camfield, 1980). For M_w equal to 9.0, we obtain a value for H of 22.5 m. Amplitudes of 68.1 and 78 cm were estimated from the arrival sequences at the bottom pressure recorders yielding amplitudes at the source of 21.3 and 27.5 m for BPRs 21401 and 21413, respectively. Although a value of 21.3 m is relatively close to the predicted value, a value of 27.3 m appears high and could reflect phase interference in the primary signal, errors accrued because the effects of refraction were not taken into account, or that the empirical relation used to obtain the first-guess provides only a rough estimate of the true value.

b. Propagation of the Tsunami across the Pacific

To a first approximation, the tsunami generated by the Great Tohoku earthquake has been assumed to follow a great circle trajectory as shown in the upper panel of Fig. 2. To test the validity of this assumption we have compared the observed travel time between the epicenter and the MARS array, with that obtained by calculating $S/\sqrt{g\overline{H}}$, where S is the great circle distance, $\overline{H}$, the mean depth along the great circle path, g, the acceleration of gravity, and $\sqrt{g\overline{H}}$ represents the shallow-water phase speed for non-dispersive waves. The bathymetry along the great circle trajectory is shown as a depth profile in the lower panel of Fig. 2. The mean depth, $\overline{H}$, is 4825 m (horizontal red line).

The observed travel time was approximately 9 hours and 50 minutes, and the calculated travel time over a distance of 8012.3km was 10 hours and 7 minutes, or about 2.7% longer than the observed travel time. Similar comparisons in the past have shown that in some cases the observed travel times are shorter than the calculated travel times, and in others, the reverse. Finally, our calculated travel time is very close to the value obtained from the National Geophysical Data Center's travel time map for the tsunami, which does include the effects of refraction. Their analysis yielded a value of 10 hours and 4 minutes (www.ngdc.noaa.gov/hazard/honshu_11mar2011/).

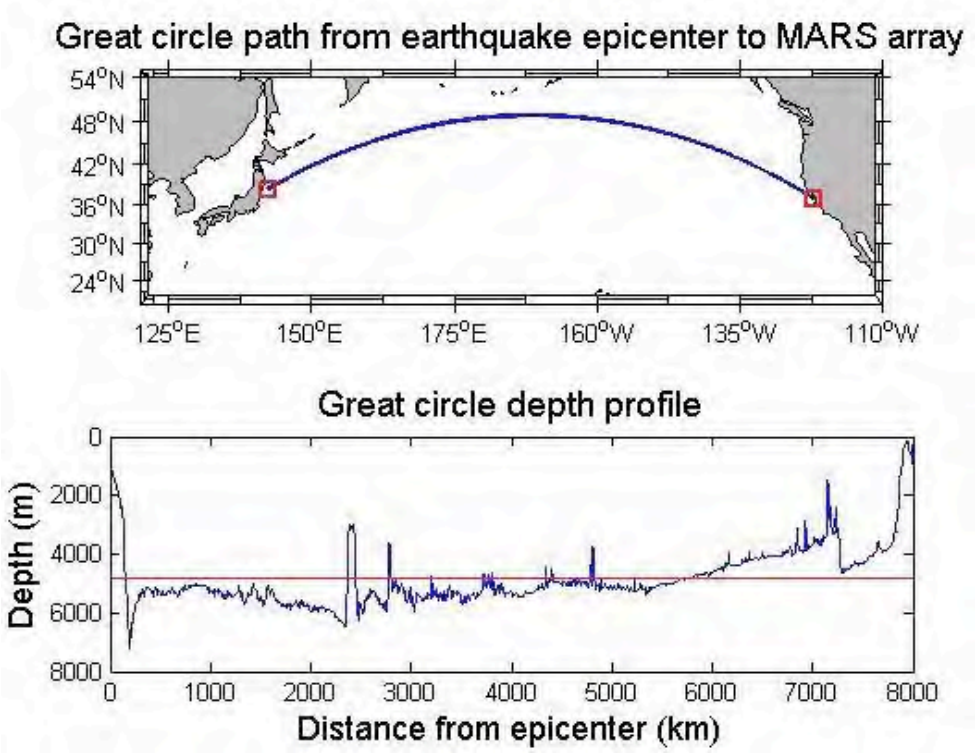

Fig. 2. The upper panel shows the great circle track from the earthquake epicenter to the MARS array located just beyond the entrance to Monterey Bay. The lower panel shows the depth profile along the great circle track. The horizontal red line corresponds to a mean depth of 4825m along the entire track.

c. The Tsunami Prior to Entering Monterey Bay

Fig. 3 (upper panel) shows the tsunami as observed at the MARS array before it entered Monterey Bay. We do not often have the opportunity to observe tsunamis in the absence of coastal influences because most tide gauges that record these events are located along the coast. The predicted period of the tsunami, T, can be approximated by $log_{10} T = 0.625 \cdot M_w - 3.31$, yielding a value of about 135 minutes (Wilson and Torum, 1968). As we look at the arrival sequence at least three well-defined peaks occur within this period, consistent with the JMA analysis. The first peak, and by far the largest, has an amplitude of approximately 25 cm. The largest aftershocks may have also generated secondary

tsunamis that contributed to the arrival sequence. Although only the first 12 hours of the arrival sequence are shown, it continued for at least five days before settling down to background levels. Because major peaks in the wave train occurred for many hours after the first arrival, the extended arrival sequence contains transoceanic reflections of the main event from many locations around the North Pacific basin (Murty, 1977). Overall, the reverberation times following such an event are expected to be on the order of a week (Munk, 1963).

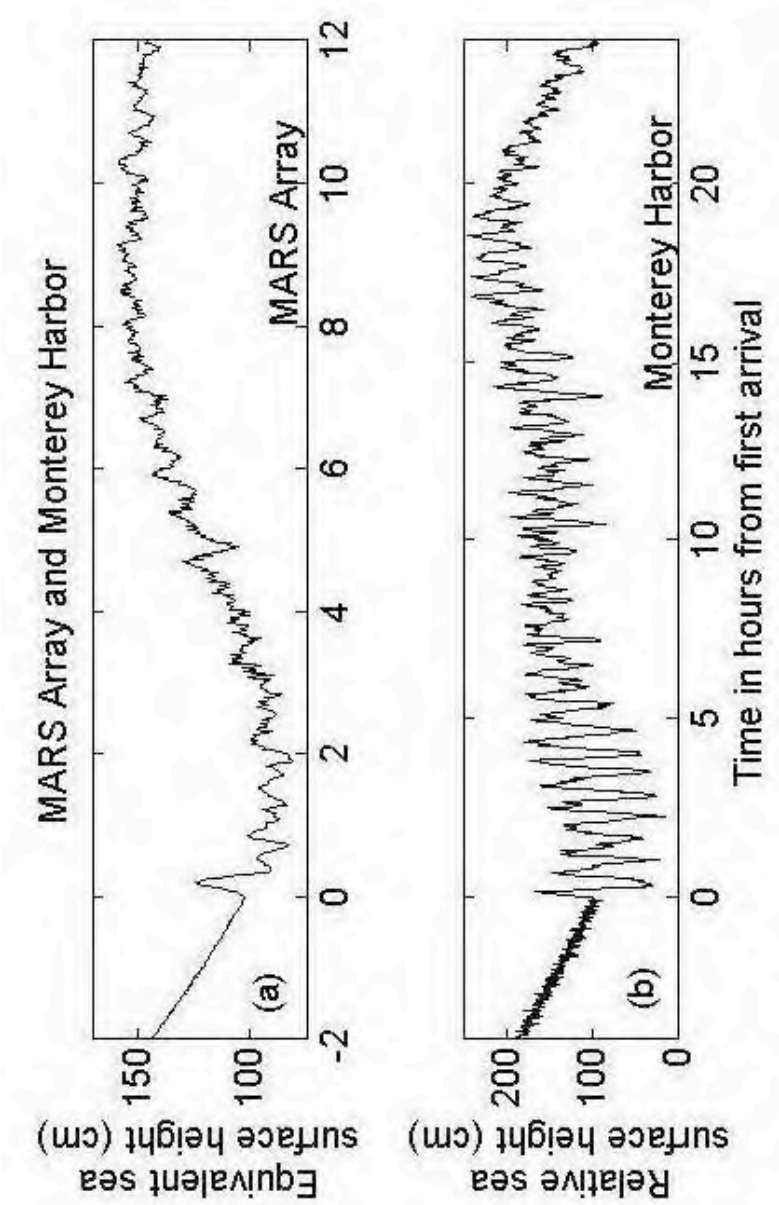

Fig. 3. The upper panel shows the pressure signal (converted to equivalent surface elevation) recorded at the MARS array for the tsunami generated by the Great Tohoku Earthquake starting two hours before the first arrival. The lower panel shows one-minute water levels recorded at the tide gauge in Monterey Harbor starting four hours before the first arrival.

On closer inspection, the trace also contains a 3-4 minute oscillation that is superimposed on the wave train starting about two hours into the arrival sequence. This oscillation may be due to interaction of the tsunami with the ridge upon which the pressure transducer is located. To explain in more detail, there are basically two different types of oceanic oscillations, oscillations of the First Class (OFC), also referred to as Gravoid modes that exist with or without the rotation of the earth, although their frequencies are modified due to earth rotation and gravity appears explicitly in their frequency equation (Murty and El-Sabh, 1986). These have periods of the order of a few minutes to several hours, depending upon the geometry of the water body and the bathymetric gradients. Oscillations of the Second Class (OSC), often called rotational modes (Elastoid-inertia modes), owe their existence to the rotation of the earth and gravity does not play a significant role in the frequencies they represent. OFC and OSC are separated in frequency by the so-called Pendulum day, which depends upon the latitude, with OFC having periods smaller then the Pendulum Day and OSC having periods greater than the Pendulum Day.

A similar situation occurred during the Indian Ocean tsunami of December 26, 2004 where oscillations of both OFC and OSC types were identified in sea level observations along the coastlines of India (Nirupama et al., 2005a; Nirupama et al., 2005b). In the present case, however, it appears that the 3-4 minute period oscillations are of the OFC type because of their relatively short period, i.e., less than a Pendulum day, and arose when the tsunami wave encountered the steep bathymetric gradients leading up to the MARS array. Such gradients that occur on coastal shelves, shelves around islands, seamounts, ridges and valleys, have been shown to generate short-period waves of the types described above during other tsunamis as well (e.g., Neetu et al., 2011).

d. The Tsunami Transformation after Entering the Bay

Once the tsunami entered Monterey Bay, it was transformed into a series of resonant oscillations often called seiche modes. This process is well-known and has been studied in some detail in Monterey Bay (e.g., Breaker et al., 2010). The lower trace in Fig. 3 (lower panel) shows the broadband response based on one-minute sampling of water levels from the tide gauge in Monterey Harbor (Fig. 1). According to our observations, the amplitude of the first arrival in the sequence has an amplitude of approximately 75cm, close to the value reported by the Pacific Tsunami Warning Center (70cm). Amplitudes inside the bay far exceed the amplitude of the tsunami outside the bay due to the excitation of resonant modes of oscillation whose periods are dictated by the boundaries that constrain them.

Returning to Singular Spectrum Analysis (SSA) as described in Section 2, the method was used to decompose the tidal record from Monterey. First, SSA was used to remove the diurnal and semidiurnal tides with a window length of 1000 minutes. The residuals were then subjected to a second SSA using a window length of 160 minutes. The reconstructed modes corresponding to the five largest eigenvalues are shown in Fig. 4. The modes are shown in order of decreasing period from top to bottom. The primary mode of oscillation is shown in the second panel. This highly resonant mode, as indicated by the purity and regularity of the waveform, has a period of 36-37 minutes, and corresponds to the transverse mode of oscillation that assumes a nodal line across the entrance of the

bay (Fig. 1). This oscillation corresponds to quarter-wave resonance and was observed previously for the Great Alaskan Earthquake of 1964 (Breaker et al., 2009). Both tsunamis entered the bay from the northwest. This mode also reveals a modulation period of slightly over 12 hours and so may reflect the influence of the semidiurnal tide.

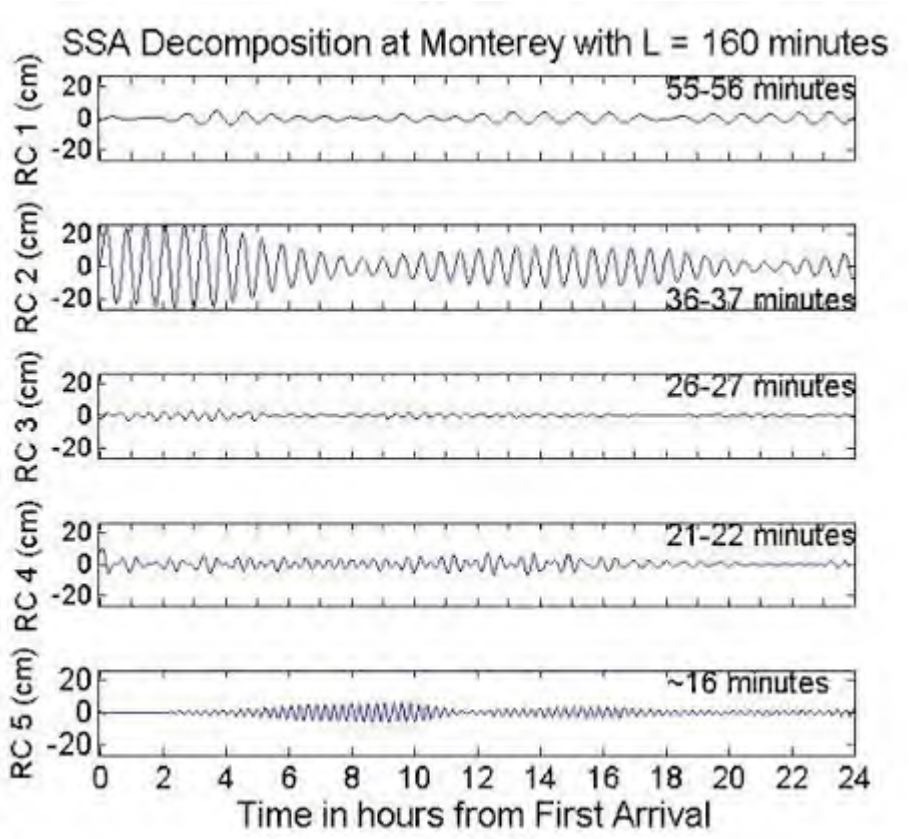

Fig. 4. This figure shows a Singular Spectrum Analysis (SSA) decomposition of the one-minute water level data from the tide gauge into a sequence of five independent modes for the first 24 hours following the first arrival. The label, "RC", on the vertical axis refers to "Reconstructed Component".

The top panel shows an oscillation with a period of 55-56 minutes and corresponds to the longitudinal mode for Monterey Bay and has been observed on numerous occasions. We note that there was a delay of almost two hours before this mode was fully excited. The third panel shows a weak response for the mode with a period of 26-27 minutes, a mode that has likewise been observed in the past. The fourth panel shows a frequently observed mode with a period of 21-22 minutes. Finally, the fifth panel shows a highly resonant oscillation with a period of approximately 16 minutes, a mode that was not fully excited until several hours into the sequence.

Previous studies have shown that all of the modes except for the longitudinal mode (top panel) have higher amplitudes in the southern part of the bay near Monterey and at the north end of the bay near Santa Cruz. Higher amplitudes at the north end of the bay undoubtedly contributed to the extensive damage that occurred in Santa Cruz Harbor.

4. SUMMARY AND CONCLUSIONS

The tsunami-generated wave before it entered Monterey Bay contained an oscillation with a period of 3-4 minutes that was most likely generated by interaction of the incoming wave as it approached the ridge where the MARS array is located, and the local bathymetry. The response of Monterey Bay to the tsunami in terms of its resonant behavior was primarily characterized by quarter-wave resonance with a period of 36-37 minutes, corresponding to the bay's transverse mode of oscillation. Although other modes of oscillation were excited their responses were overshadowed by the primary response.

The response to the tsunami generated by the Great Tohoku Earthquake in terms of the damage incurred inside the bay was extensive but confined to Santa Cruz Harbor. For the purpose of issuing warnings, for tsunamis that enter the bay from the northwest which will be the case for most earthquakes that are generated along the Pacific Rim from Japan to the Gulf of Alaska and down the west coast of North America, it is likely that Santa Cruz Harbor could again experience significant damage for events whose magnitudes approach those of the Great Tohoku and Great Alaskan earthquakes.

5. ACKNOWLEDGMENTS

We thank Cary Wong from NOAA's National Ocean Service for providing the one-minute water level data from Monterey, and William Chadwick for providing the bottom pressure data from the MARS array through the courtesy of Oregon State University and NOAA/PMEL, with funding from National Science Foundation grant OCE-0826490. We also thank Paula Dunbar from the National Geophysical Data Center for the travel time estimate presented in section 4. Finally, we gratefully acknowledge eyewitness accounts of the wave impacts on Monterey, Moss Landing and Santa Cruz Harbors from Steve Scheiblauer, Lee Bradford, and Dan Haifley.

6. REFERENCES

Breaker, L.C., Y.-H Tseng, and X. Wang (2010), On the natural oscillations of Monterey Bay: Observations, modeling, and origins. Progress in Oceanography, 86, 380-395.

Breaker, L.C., T.S. Murty, J.G. Norton, and D. Carroll (2009), Comparing the sea level response at Monterey, California from the 1989 Loma Prieta earthquake and the 1964 Great Alaskan Earthquake. Science of Tsunami Hazards, 28, 255-271.

Camfield, F.E. (1980), Tsunami Engineering. Special Report No. 6, U.S. Army Corps of Engineers, Coastal Engineering Research Center, Fort Belvoir, VA, 222 pp.

Ko, D.S. (2009), DBDB2 v3.0 Global 2-minute Topography. http://1117320.nrlssc.navy.mil/DBDB3_WWW. Naval Research Laboratory, Oceanography Division, Ocean Dynamics and Prediction Branch.

Munk,W.H. (1963), Some comments regarding diffusion and absorption of tsunamis. In: D.C. Cox (ed.). Proc. tsunami meetings associated 10th Pac. Sci. Congr. , Honolulu, Hawai. Union Geod. Geophys. Monogr. 24. pp. 53-72.

Murty, T.S. (1977), Seismic Sea Waves – Tsunamis. Bulletin 198, Department of Fisheries and the Environment Fisheries and Marine Service. D.W. Friesen & Sons, Ltd, Altona, Manitoba, Canada.

Murty, T.S. and M.I. El-Sabh (1986), Gravitational oscillations in a rotating paraboloidal basin: a classical problem revisited. Mahasagar (Bull. Of the National Inst. of Oceanography, Goa, India), 18(2), 99-127.

Neetu, S., I. Suresh, R. Shankar, B. Nagarajan, R. Sharma, S.S.C. Shenoi, A.S. Unnikrishnan, and D. Sundar (2011), Trapped waves of the 27 November 1945 Makran tsunami: observations and numerical modeling. Natural Hazards, DOI 10.1007/s11069-011-9854-0.

Nirupama, N., T.S. Murty, A.D. Rao and I. Nistor (2005a), The Role of Gravoid and Elastoid Modes in oscillations around Andaman and Nicobar Islands. In Indian Ocean Tsunami, Ed: V. Sundar, Indian Institute of Technology Madras, India, 41-52.

Nirupama, N., T.S. Murty, A.D. Rao and I. Nistor (2005b), Tsunami in Andaman and Nicobar Islands: Oscillations of the First and Second Class. In Indian Ocean Tsunami, Ed: V. Sundar, Indian Institute of Technology Madras, India, p. 22-30.

Vautard, R., P.Yiou, and M. Ghil (1992), Singular spectrum analysis: A toolkit for short, noisy chaotic signals. Physica D, 58, 95-126.

Wilson, B.W., and A. Torum (1968), The tsunami of the Alaskan earthquake, 1964: Engineering evaluation. U.S. Army Corps. Eng. Coastal Eng. Res. Cent. Tech. Memo 25, 401 pages.

ISSN 8755-6839

SCIENCE OF **TSUNAMI HAZARDS**

Journal of Tsunami Society International

Volume 30 **Number 3** **2011**

TSUNAMI RISK MITIGATION THROUGH STRATEGIC LAND-USE PLANNING AND EVACUATION PROCEDURES FOR COASTAL COMMUNITIES IN SRI LANKA

Woharika Kaumudi Weerasinghe[1], Akihiko Hokugo[2], Yuko Ikenouchi[3]

[1]Researcher, Research Center for Urban Safety and Security, Kobe University, Japan
[2]Professor, Research Center for Urban Safety and Security, Kobe University, Japan
[3]Graduate Student, Research Center for Urban Safety and Security, Kobe University, Japan
woharika@hotmail.com[1]

ABSTRACT

Safety measures against the future disaster risk are considered as the main aspect of post disaster reconstructions. The majority of post-disaster villages/settlements and due projects on Sri Lankan coastline are apparently lacking behind the proper safety measures and adequate evacuation procedures. Therefore the immediate necessities of proper safety measures have to be emphasized in order to mitigate future tsunami risks. This paper introduces a number of post disaster coastal villages/settlements, which are in future coastline hazard risk, mainly in a future tsunami event. These include their location risk, land uses and housing designs defects and shortcomings of other safety measures. Furthermore few tsunami risk mitigation measures through land use planning strategies, which could be applied more easily in community level, are introduced. In addition to those the strategic development methods of functional networks of evacuation routes and shelters in different topographies are examined.

Keywords: *Tsunami Risk Mitigation, Coastal Communities, Strategic Land-use Planning, Evacuation Routes, Vertical Evacuation Shelter*

1. INTRODUCTION

Dealing with tsunami risk mitigation measures is a relatively complex task. Tsunamis may extremely destructive in unexpected occasions although they are considered as infrequent events. That non-neglectful destructiveness and vulnerability was demonstrated in 2004 Sumatra earthquake and tsunami[1] by claiming more than 35,000 peoples' lives and affecting two thirds of the entire Sri Lankan coastline. Affected coastal area stretching over 1,000 kilometers and approximately 80,000 houses were completely destroyed and more than 40,000 partially impacted (ADB, 2005). Since then a number of post disaster reconstruction projects[2] have been implemented by the Sri Lankan government and many other national and international organizations still on the process of re building those affected coastal communities.

Although safety measures against the future disaster risk are considered as the main aspect of post disaster reconstructions, majority of the post-disaster villages/settlements in southern coastline have been established without proper safety measures or adequate evacuation procedures. Most of the ongoing coastline projects have being repeating the past mistakes of unsafe planning and construction. At the same time new residential areas which are yet to be planned for northern and eastern coast line communities are at risk due to lack of procedures of safety planning and building guide lines.

Those problems have easily been identified during our field visit at the most affected areas, dated from 07/08/2010 to 16/08/2010. Such mistakes may increase the susceptibility of coastal communities to unprecedented, extensive damages in such event of future natural disasters, hence immediate solutions are required. It seemed that lack of experience and information on handling the post-tsunami situations, unavailability of proper disaster resistant construction and land use planning guide lines have become the critical factors. Failure to implement such obvious safety aspects can never be justified for not being able to plan reasonably and practically, as such issues have been highly disadvantageous for the post disaster reconstruction process in Sri Lanka. Inclusion of DRR (Disaster Risk Reduction) as an integral element in every phase of planning for reconstruction and combination of community and living environment development proposals within the context of safety planning have now become the major challenges in the field of post disaster reconstructions in the country.

2. OBJECTIVES

The main objective of this study is to achieve the research targets of developing a comprehensive strategic plan compiles all components of the planning which extensively addresses such safety planning and evacuation procedures for Sri Lankan coast line and creating a combination of community and living environment development proposals within the context of safety planning.

To introduce a number of post disaster coastal villages/settlements, which are at future tsunami risk including their location risk, land uses and housing designs defects and shortcomings of other safety measures.

To propose few tsunami risk mitigation measures through land use planning strategies, which could be applied in community/village level more easily.

3. IMPORTANT OF PLANNING IN DRR

Planning as a process is inevitable in a reconstruction scenario, whether the decision is to just rebuild houses or to achieve comprehensive development resilient to the future disasters (World Bank 2010)*. On the implementation, the detail level of planning process and enabling or impeding of planning in reconstruction process will become major issues in future disaster events. The correct planning processes consider DRR for organizing housing and infrastructure reconstruction, addressing the impacts of the disaster and disaster risk reduction.

Further post disaster planning provides an opportunity to modify existing policies, inappropriate/unsafe legislation and regulations, strengthening institutions and improving construction methods as the basis of reconstruction forms by laws, regulations, plans and institutional frameworks.

3.1. Current Land Use Planning and Necessity of Proper Land Use Changes

It is hard to identify the proper DRR guidelines or clarification of disaster vulnerable zones in National Physical Planning Guidance or in the latest report of National Physical Planning on "Land Use Changes That Have to Taken Place in Sri Lanka" in year 2001**. The problems which could be risen up through inadequate planning guidance such as difficulties in identification of low risk zones for site selection, propose of appropriate structural designs due to inundation risk levels have been come across in most of the project planning and implementations. Those problems have been identified through several official visits by the relevant government authorities[3]. Further the unclear view of coastal communities regarding the safe areas and evacuation routes were identified through number of interviews.

Such insufficient considerations of coast line natural hazards and unavailability of risk mapping in comprehensive land use planning system in Sri Lanka emphasis the necessity of appropriate plans that follow tsunami readiness. The incorporation of zoning laws which guides for safe relocation for the existing system considering tsunami risk simulations and inundation levels will be more functional.

3.2. Village/Community Level Strategic Land-use Planning and its Importance

Fig.1. Introduction of Village/Community Level Strategic Land-use Planning

We suggest that the strategic land use planning which properly addresses DRR aspects and ready to place in action in a short time period as the best, simple, affordable, local and long term solution for Sri Lankan coastal areas. It offers a fruitful approach in complex task of tsunami risk mitigation measures more easily for the existing coastal villages/settlements and for the areas to be developed along with few moderations.

Comprehensive Land use plan addresses the overall and long-term issues of the community and establish a framework for the physical development of a region, municipality, city or village. In this study comprehensive planning is defined as a planning process that incorporates land use planning and physical planning. In this paper we focus on village and community level strategic land-use planning which comes under land-use planning and development of tsunami risk mitigation measures only. (Fig.1)

4. TSUNAMI RISK MITIGATION MEASURES

Land-use changes, relocation, development of water barriers, elevated sites and evacuation routes and shelters have been introduced as main tsunami risk mitigation measures though land-use planning in this paper.

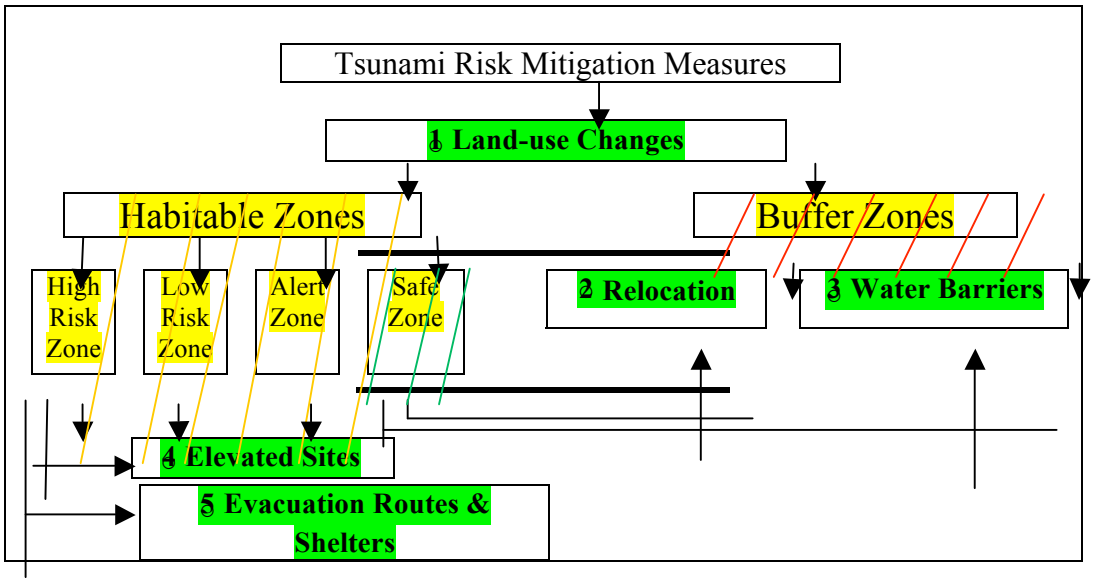

Fig. 2. Tsunami Risk Mitigation Measures

4.1. Introduction of DRR Land-use Changes to Existing Land-use planning

4.1.1. Introduction of accurate tsunami resist and non resist areas (Habitable Zones and Buffer Zones)

Although a Buffer Zone regulation[4] with construction restrictions has been introduced to cost line it does not seem to be working effectively in most of the areas as the reconstruction of permanent or

temporary shelters of tourist industry owners/ fishery community, etc. can be seen. Further many buildings projects has not been in accordance with the current tsunami resistant structural considerations, designs etc. and many yet to be constructed even in buffer zone through especial construction permissions and exemptions for tourist industry promoters while non-existence situation of planning or building guide lines.

On the other hand buffer zone regulation was not originally for demarcate a tsunami hazard zone, but for the conservation of coastal environment enacted by Coastal Conservation Department (CCD)*** which depicts the shortcomings of insufficient assessments of past tsunami hazards or estimation of future ones during its enactment.

It is suggested that following steps will be helpful to identify more accurate habitable safe coastal areas (Habitable Coastal Zone), and non-habitable unsafe coastal areas (Buffer Zone).

a- Estimate of inundation; Through an assessments of past inundated areas and projection/simulation of future inundation areas
b- Assessment of damage; Through an assessments of damage by past tsunamis and projection/simulation of damage by future tsunamis
c- Assessment of current levels of tsunami preparedness

4.1.1.1. Habitable Coastal Zone

a.) Minor Zoning through a risk assessment
Safety can be ensured by conducting a minor zoning in accordance with High Risk Zone, Low Risk Zone, Alert Zones and Safe Zone, which can facilitate in establishing early warning system and evacuation procedures.
b.) Promotion of Strategic Area Arrangements
The future risk can be mitigated through strategic area arrangements in habitable zones. Ex. Movement of Residential/Commercial areas to Low risk zones and Manufacturing/ Marine areas to High-risk zones.

4.1.1.2. Buffer Zone

The buffer zones can be used as barrier areas by developing artificial water barriers (wall) or natural water barriers (green belt).

4.2. Relocation

Relocation at every possibility is the most safest and economical measure which could be applied for the communities in high risk or buffer zones. It can be a tough job but still practical enough to counter post relocation problems, if proper planning including prior identification of safe zones is achieved.

4.2.1. Post Relocation Problems

We could identify number of post relocation problems in southern coastline as follows.

- Unavailability of future disaster responses; the relocation sites that have been selected without proper risk assessment or simulation can still have future disaster risk.

- Livelihood problems; mainly the fishery community is facing the livelihood problems due to the lottery system followed by the authorities for the distribution of permanent houses other than distance level, prior to livelihoods. This has caused returning to unsafe temporary shelters in coastline.

- Reluctance of distance living and return; disappearances of original community order, unwillingness or mental trauma to settle in a completely different inland settlement were the other main reasons for the reluctance of beneficiaries to settle in a distance relocation settlement and return to coastline except the livelihood problems.

- Inability of creating harmony with existing environment; many reconstructions of the permanent housing have not yet been able to act together with existing regional or local patterns and quality, thus creating the conflicts and gaps between the inhabitants and new comers.

4.2.2. Considerations in Relocation

Safe site selection due to a proper risk assessment or simulation method, Site selection prior to livelihoods, Preservation of the maximum original communities' order in new settlements, Keeping harmony with existing settlements, Active participation of beneficiaries, in relocation process could be effective to establish more safe, strong and long term relocated communities.

4.3. Physical Water Barriers

Protection of existing natural water barriers such as sand dunes and green belts or creation of those could minimize the impact and inundation level of tsunamis.

Fig. 3.Disturbed Natural Sand-dunes in Hambantota District

4.4. Elevated Sites for Constructions

Creation of elevated sites for constructions in high economically valued or essential land areas could reduce the effect of tsunami waves in future events.

4.5. Functional Networks of Evacuation Routes, Vertical Evacuation Shelters and Existing Safe Escape Places

Since evacuation is one of the most important codes in the disaster occasions, developing functional networks of evacuation routes, vertical evacuation shelters and identification of existing safe escape places are highly necessitated. On the other hand development of evacuation routes will lead proper access to the areas while construction of vertical evacuation shelters leads to public facilities development with strategic building proposals such as shopping complex, community centers, cultural centers, observation towers. Furthermore these kinds of development proposals lead to combine community and living environment development proposals within the context of safety planning.

a.) Use of Zoning: Use of zoning in proposed warning levels could be more systematic.

b.) Establishment of easy, understandable short and long distance evacuation shelters with escape routes in community and GN Division[5] level: The aspect of developing the evacuation route network should be coherent with proper evacuation sites, designation of evacuation routes, distribution of evacuation sites, location of evacuation routes, topography of evacuation sites, evacuee capacity, evacuation areas (including their relationship to residential zones), evacuation site structures, readying the approach routes, road width, potential problem spots (bridges, tunnels, etc.) In addition an evaluation of the evacuation feasibility of sites and routes should be done.

c.) Identification of existing tsunami resistant buildings: Community level pre introduction of each building could be more favorable in a disaster occasion.

5. DEVELOPING FUNCTIONAL NETWORKS OF ESCAPE ROUTES AND VERTICAL EVACUATION SHELTERS FOR SELECTED CASES ON SOUTHERN COASTLINE OF SRI LANKA

We have selected three coastline reconstructed housing settlements (case 1, 2 and 3) and one original community (case 4) which are in future tsunami risks as per the case studies. In this study we have attempted to observe the location/topographic risk and evaluate the proposed zoning, warning levels, evacuation modes, evacuation routes and evacuation shelters accordingly.

Zoning has been done by considering only past records of inundation levels and interviews with community members. Warning levels, evacuation modes, evacuation routes and evacuation shelters have been proposed with the use of site visits records, interviews with community members andGoogle earth maps[6] only.

Fig. 4. Locations of Case Studies

Table 1: Development of Functional Network of Evacuation Procedures for Selected Cases in Southern Coastline of Sri Lanka.

Tasks		**Case 1** French Village	**Case 2** Pelena Housing	**Case 3** Thotamuna & Polhena	**Case 4** Mirissa Harbor area
A.) **A.) Zoning** 1. High Risk Zone (FWL) (for this study 0-500m)		Highly demands (risky topography)		Highly demands (risky topography & high dense area)	
2. Low Risk Zone (FWL) (for this study 500-1000m)		critical	difficult to demarcate	easy to demarcate	
3. Alert Zone (FWL & SWL) (for this study 0-200m)		river banks		river banks	Not found
4. Safe Zone (SWL) (for this study 1000m~)		average time to reach	long time to reach	short time to reach	average time to reach
B.) Warning Levels 1. First Warning Level –FWL		- People in High Risk Zone and Alert Zone should be evacuated to Low Risk Zone or safe vertical shelters - People in Low Risk Zone should be evacuated to Safe Zone or safe vertical shelters			
2. Special Warning Level –SWL		- People in Safe Zone should be evacuated to safe vertical shelters			
C.) Evacuation Modes	High Risk Zone	On foot			
	Low Risk Zone				
	Alert Zone				
	Safe Zone	Vehicles allow			
D.) Evacuation Routes		- clear directions with sign boards - pre defined routes at every possibility - Alternative roads for alert areas and risky points (river banks, bridges, etc.)			

E.) Evacuation Shelters	High Risk Zone	- need future construction proposals: Tsunami resistant multi storied buildings within short distances
	Low Risk Zone	- use of existing buildings: Appropriate buildings such as community centers, hotels, schools, etc.

5.1 Case 1-French Garden Village-Galle District

Living environment, housing arrangement and location of the settlement 1:200	Views of the widely pen sea front of the settlement	Reconstructed unsafe single storied houses in the settlement

Fig. 5: Surrounding and Inside Views of the Reconstructed "French Garden Village" Housing Settlement

The location risk could be identified due to wide-open sea front and adjacent river without any tsunami wave breakers. The non tsunami resistant single storied houses and unavailability of adequate evacuation routes and shelters can certainly increase the affects of future tsunamis. Proposal of zoning and evacuation routes and shelters development for the communities of Kataluwa area are shown in Fig. 6.

Fig. 6: Proposal of Zoning, Evacuation Routes and Shelters for "French Garden Village" and Surrounding Communities in Kataluwa-west GN Division, Galle District.

5.2 Case 2-Pelena Solidealstar Village-Galle District

Living Environment, housing arrangement and location of the settlement, Scale: 1:200	Views of two storied houses and community center in the settlement	Two storied houses adjacent to fully damaged houses

Fig.7: Surrounding and Inside Views of the Reconstructed "Pelena Solidealstar Village" Housing Settlement

Fig. 8: Proposal of Zoning, Evacuation Routes and Shelters for "Pelena Solidealstar Village" and Surrounding Communities in Pelena GN Division, Galle District.

The Pelena Housing settlement and other surrounding communities are in a risk location due to the adjacent sea and river, without sufficient water barriers in a future tsunami. It has been attempted to mitigate the future effect by constructing reinforced two-storied housing but still a considerable amount of risk remains due to design problems related to creating proper safe places. Furthermore unavailability of adequate evacuation routes and shelters has increased the disastrous effects of

tsunami in a future event. Fig. 8 shows the proposals for zoning and development of evacuation routes and shelters for the communities of Pelena area.

5.3 Case 3-Thotamuna and Polhena Owner Driven Housing Project-Matara District

In the areas of Polhena and Thotamuna, which were severely affected by the last tsunami, some reconstructed multi storied houses with pillar structures can be found as a tsunami risk mitigation method (Fig. 9). Existence of famous recreation beach and fish market which make the area crowded in daily life emphasize the necessity of efficient evacuation routes and shelters in a future disaster occasion. The proposal for zoning and evacuation routes and shelters development is shown in Fig.10

Living environment, housing arrangement and location of Thotamuna 1:200	Reconstructed three and two storied houses in the affected villages	Living Environment, housing arrangement and location of Polhena 1:200

Fig. 9: Views of the **"**Thotamuna and Polhena" Owner Driven Housing and Locations

Fig. 10: Proposal of Zoning, Evacuation Routes and Shelters for "Thotamuna and Polhena" Owner Driven Housing and Surrounding Communities in Thotamuna and Polhena GN Division, Matara District.

5.4 Case 4-Unsafe Coastal Housing in Mirissa-Matara District

Living Environment, housing arrangement and location of the housing area, Scale-1:200	Damaged houses by Sumatra tsunami 2004	One of the unsafe houses in the area; located about 40m from the sea

Fig. 11: Views of the Existing Unsafe Housing and Surrounding Area Adjacent to Mirissa Fishery Harbor

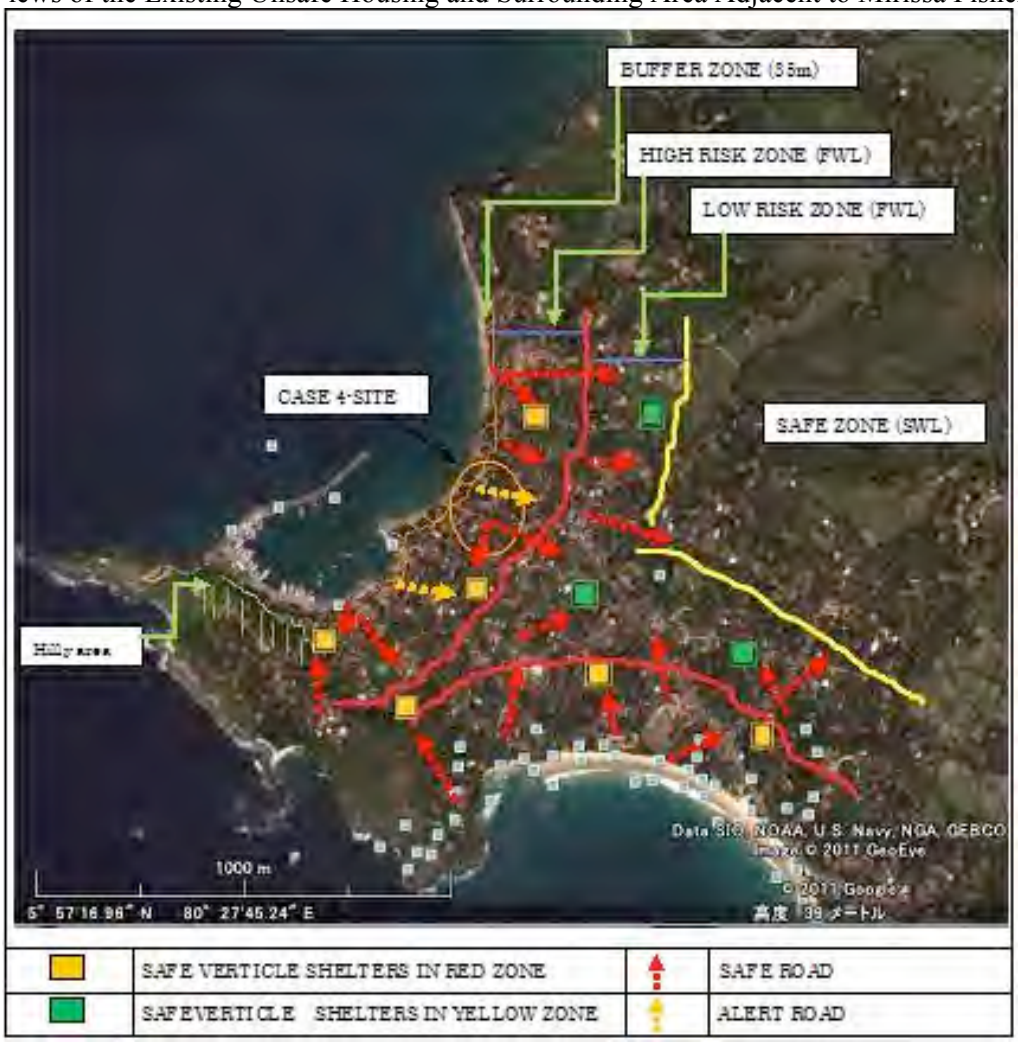

Fig. 12: Proposal of Zoning, Evacuation Routes and Shelters for Unsafe Housing Area Adjacent to Mirissa Fishery Harbor and Surrounding Communities in Mirissa-south GN Division, Matara District.

It is complicated to find any tsunami risk mitigation method adopted by the present coastline communities in Mirissa and surrounding areas, although extensive damages were recorded during the past tsunami. The buffer zone reduction up to 35m has remained the partially or non-affected houses at the coastline without proper protection or evacuation guidance. Fig.12 shows the proposals for zoning and development of evacuation routes and shelters in the area.

6. CONCLUSIONS

1. Changes of land-use planning which address DRR and combination of tsunami risk mitigation measures and safety evacuation procedures to the existing planning system will mitigate the future disaster risk and lead to more safe coastal communities.
2. The use of land and zoning laws, guidance for relocation to safer zones are in cooperation with the changes for the existing system, which considers tsunami risk simulations, and inundation levels could be more functional.
3. Strategic development of evacuation routes and vertical shelters will mitigate the future disaster risk while leading to a sound combination of the community and living environment development proposals within the context of safety planning.
4. There is a necessity of disaster mitigation management plans, which consider the topography of the each area.
5. A post disaster planning process, which incorporates active collaboration among the disaster mitigation agencies, all the reconstruction agencies consist with private sector, other stakeholders and the affected communities, leading to develop the safe and sustainable coastal communities.

Acknowledgements

This study is supported by a research fund awarded to Research Center for Urban Safety and Security, Kobe University, Japan.

REFERENCES

1.) Guidebook for Tsunami Preparedness in Local Hazard Mitigation Planning, National Land Agency, Ministry of Agriculture, Forestry & Fisheries Structural Improvement Bureau, Fisheries Agency, Ministry of Transport, Japan Meteorological Agency, Ministry of Construction, Fire and Disaster Management Agency, pp.55-70, pp.86-91

2.) Guidelines for Housing Development in Coastal Sri Lanka, Statutory Requirements and Best-Practice Guide to Settlement Planning, Housing Design and Service Provision with Special Emphasis on Disaster Preparedness, Tsunami Disaster Housing Program, National Housing Development Authority, Ministry of Housing and Construction, Colombo, Sri Lanka, 2005

3.) *** Gazette Extraordinary of the Democratic Socialist Republic of Sri Lanka, Part 1 Sec (1), 2006 http://www.coastal.gov.lk/czmp%20english.pdf

4.) ****Janaka J. Wijetunge, Tsunami on 26 December 2004: Spatial Distribution of Tsunami Height and the extent of Inundation in Sri Lanka, Journal of Science of Tsunami Hazards, Vol. 24, No. 3, pp. 225-239, 2006

5.) **Land Use Changes in Sri Lanka, Background Information for Preparation of National Physical Planning Policy, Percy Silva, Centre for National Physical Planning [CNPP], Urban Development Authority [UDA], National Physical Planning Department [NPPD], Report No.03, August 2001

6.) *Safer Homes, Stronger Communities: A Handbook for Reconstruction after Natural Disasters, Abhas K. Jha, Jennifer Duyne Barenstein, Priscilla M. Phelps, Daniel Pittet, Stephen Sena, World Bank, pp.109 -129, 2010

7.) Tsunami Evacuation Plan for Sanur Bali, Bali, A Documentation of the Process and Results of Tsunami Evacuation Planning, District Government of Denpasar, BPBD Denpasar, Bali Hotel Association (BHA), The Indonesian Red Cross, Bali Chapter, Kelurahan and villages authorities, Sanur Development Foundation, GTZ IS – GITEWS, May 2010

8.) Woharika Kaumudi Weerasinghe, Akihiko Hokugo and Yuko Ikenouchi, Tsunami Risk Mitigation Measures Identified through Strategic Land Use Planning for Coastal Areas in Sri Lanka, An International Symposium on Earthquake Induced Landslides and Disaster Mitigation at the 3rd Anniversary of the Wenchuan Earthquake, Chengdu University of Technology, China, May 12-15 2011.

9.) Woharika Kaumudi Weerasinghe, Akihiko Hokugo, Tsutomu Shigemura and Ryosuke Aota, An Examination of Two Post Disaster Housing Reconstruction Approaches of Sri Lanka, An international Symposium on Sustainable Community ISSC, Forwards Making Space for Better Quality of Life, Indonesia, 2009.

10.) Woharika Kaumudi Weerasinghe and Tsutomu Shigemura, A Study on Transformation of Living Environment and Domestic Spatial Arrangements: Focused on a Western Coastal Housing Settlement of Sri Lanka after Sumatra Tsunami Earthquake 2004, Journal of Asian Architecture and Building Engineering, Vol.7 No.2, pp.285-292, Nov., 2008

Notes

[1]The Sumatra earthquake and tsunami, with a magnitude 9.0, occurred at 7.58 AM on December 26th 2004 under the Indian Ocean. As a result of the earthquake and tsunami, in all affected regions more than 220,000 people died, making it one of the greatest natural disasters recorded.

[2]The introduction of buffer zone led to two types of post tsunami housing reconstruction programs. a; Home-owner Driven Housing Reconstruction Program for fully/partially damaged hoses outside the buffer zone.
The government of Sri Lanka is providing cash grant reimbursed by different redevelopment banks and bilateral donors to an affected homeowner for reconstruction of his/her house. b; Donor-driven Housing Reconstruction Program for relocate the affected families were in buffer-zone. All affected families are entitled to a house built by a donor agency in accordance with Government of Sri Lanka standards. The donor will provide each new settlement with an internal common infrastructure while Government of Sri Lanka provides the services up to the relocation site.

[3]UDA (Urban Development Authority, Colombo), NHDA (National Housing Development Authority, Colombo), NDMC (National Disaster Management Centre, Colombo), NBRO (National Building Research Organization, Colombo), District Secretariats in Galle, Matara and Hambantota districts, Sri Lanka.

[4]The buffer zone (or set-back-zone) was divided in to two parts as; Zone 1: 100 m landwards from the mean high waterline in the western, southern and southwestern districts. Zone 2: 200 m landwards from the mean high water line in the northern and eastern districts of Sri Lanka. The buffer zone has been a critical issue in the recovery process, which has not worked equally effectively in all areas. Later on it was reduced up to minimum of 35m and currently varies in-between 35m-200m.

[5]*Grama Niladari* (Village Officer) Division of Sri Lanka. Number of GN Divisions creates a DS Division (District Secretarial Division).

[6] Maps downloaded from websites of http://www.earth.google.com

ISSN 8755-6839

SCIENCE OF **TSUNAMI HAZARDS**

Journal of Tsunami Society International

Volume 30 **Number 3** **2011**

A CATALOG OF TSUNAMIS IN LA RÉUNION ISLAND FROM AUGUST 27TH, 1883 TO OCTOBER 26TH, 2010*

Alexandre Sahal[1], Julie Morin[2], François Schindelé[3] and Franck Lavigne[1]

1. Laboratoire de Géographie Physique, Université Paris 1 Panthéon-Sorbonne, CNRS (UMR 8591), 1 Place Aristide Briand, 92195 Meudon Cedex, France.
2. Equipe « Géologie des Systèmes volcaniques », IPGP, Université de la Réunion, CNRS (UMR 7154), 15 Avenue René Cassin, BP 7151,
97715 Saint Denis, La Réunion, France.
3. CEA, DAM, DIF, Bruyères-le-Châtel, 91297 Arpajon Cedex, France.
Corresponding Author: Alexandre Sahal, alexandre@sahal.fr
*Original testimonies and high-resolution figures are available online on http://www.sahal.fr/.

ABSTRACT

The PREPARTOI project ("Prevention and research for the mitigation of the tsunami risk in the French territories of the Indian Ocean", the French acronym equivalent to « get-ready »), began in early 2010. The first stage of this integrated tsunami risk assessment project consisted in evaluating the tsunami hazard on La Réunion Island by collecting and synthesizing all available data about past tsunamis and their effects. This first step was implemented through archive and field research during 2010. Seven tsunami occurrences were identified as having impacted La Réunion Island between 1883 (explosion of the Krakatau volcano) and October 2010 (end of the field research). All these events had sources along the Indonesian margin and were triggered by earthquakes of magnitude higher or equal to Mw=7.7, affecting the island with maximal runups reaching 7m. These tsunamis mostly affected the harbors damaging many boats, especially in 2004. Although historically the tsunami hazard is quite moderate on the island's coasts, the high concentration of people along the shore and in low elevation areas, highlights considerable stakes and high vulnerability resulting in significant risk, especially in Saint-Paul, a city which was completely flooded in 1883.

Keywords: tsunamis; teletsunamis; Indian Ocean; La Réunion; catalog

1. INTRODUCTION

La Réunion Island, a French territory in the Indian Ocean, is a partly active volcanic island in the Mascarene archipelago, located northeast of Madagascar. Although the island is located in a tsunami hazardous basin, the scientific community never compiled a historical catalogue of the tsunami hazard. Only the December 26th, 2004 and the October 25th, 2010 tsunamis were investigated by field surveys (Okal et al. 2006; Sahal and Morin accepted).

In 2010, the "PREPARTOI" research program ("Prevention and research for the mitigation of the tsunami risk in the French territories of the Indian Ocean", French acronym equivalent to "get-ready", www.prepartoi.fr) began assessing the tsunami risk on the island, in response to an institutional demand for better preparedness for future tsunamis. PREPARTOI program initiated field and archive investigations to study the historical tsunami hazard of La Réunion Island. This paper presents and discusses the methods and results of this investigation.

2. METHODS

The methodology to compile this catalog is comparable to the one used recently in New Caledonia (Sahal et al. 2010). It consists in establishing a list of tsunamis that impacted territories in the Indian Ocean, as well as potentially tsunamigenic earthquakes (events of high magnitude), using on-line databases (Dunbar 2010) and previously published regional catalogs (Rastogi and Jaiswal 2006), with a critical point of view. Local earthquakes were also considered. Newspapers and administrative archives were consulted (Table 1), searching for sea level disturbance records for the selected dates (and following days).

For the more recent events, witnesses were also sought out on-site to specify and/or complete recorded observations. Through several field trips, the authors were able to calculate runup values on-site or deduce them from old maps. The physical effects were measured using the zero level of the marine charts as a reference (lowest tides).

Table 1. Consulted newspapers and archives

Tsunami event	***Newspaper***	***Observations***
25/11/1833	*Annales Maritimes et Coloniales*	NO
16/02/1861	*Annales Maritimes et Coloniales*	Unavailable
13/08/1868	*Annales Maritimes et Coloniales*	NO
	Malle (La)	NO
	Courrier de Saint-Pierre (Le)	Unavailable
	Courrier Républicain (Le)	Unavailable
	Moniteur (Le)	Unavailable
	Journal Communal de l'Île de La Réunion	Unavailable
10/05/1877	*Annales Maritimes et Coloniales*	NO
	Moniteur (Le)	Unavailable

27/08/1883	*Journal de l'Île de La Réunion*	YES
	Créole de l'Île de La Réunion (Le)	YES
	Malle (La)	YES
	Courrier de Saint-Pierre (Le)	Unavailable
	Moniteur (Le)	Unavailable
	Nouveau Salazien (Le)	Unavailable
	Port de Saint-Pierre (Le)	Unavailable
	Créole du Lundi (Le)	Unavailable
04/01/1907	*Journal de l'Île de La Réunion (Le)*	YES
	Patrie Créole (La)	YES
27/11/1945	*Progrès (Le)*	NO
	Démocratie (La)	NO
	Peuple (Le)	Unavailable
19/08/1977	*Journal de l'Île de La Réunion (Le)*	NO
	Quotidien (Le)	NO
02/06/1994	*Journal de l'Île de La Réunion (Le)*	NO
	Quotidien (Le)	NO
	Témoignages	NO
26/12/2004	*Journal de l'Île de La Réunion (Le)*	YES
	Quotidien (Le)	NO
28/03/2005	*Journal de l'Île de La Réunion (Le)*	YES
	Quotidien (Le)	NO
17/07/2006	*Journal de l'Île de La Réunion (Le)*	YES
	Quotidien (Le)	NO
12/09/2007	*Journal de l'Île de La Réunion (Le)*	YES
	Quotidien (Le)	YES
20/03/2010	*Journal de l'Île de La Réunion (Le)*	NO
	Quotidien (Le)	NO
25/10/2010	*Journal de l'Île de La Réunion (Le)*	YES
	Quotidien (Le)	YES

1. RESULTS

Seven tsunamis were identified as having impacted La Réunion Island in the past. All of them were of transoceanic origin (also called teletsunamis). Figure 1 illustrates the location of these sources as well as their local effects.

Figure 2 locates the places cited in the text. Time is expressed in 24h format.

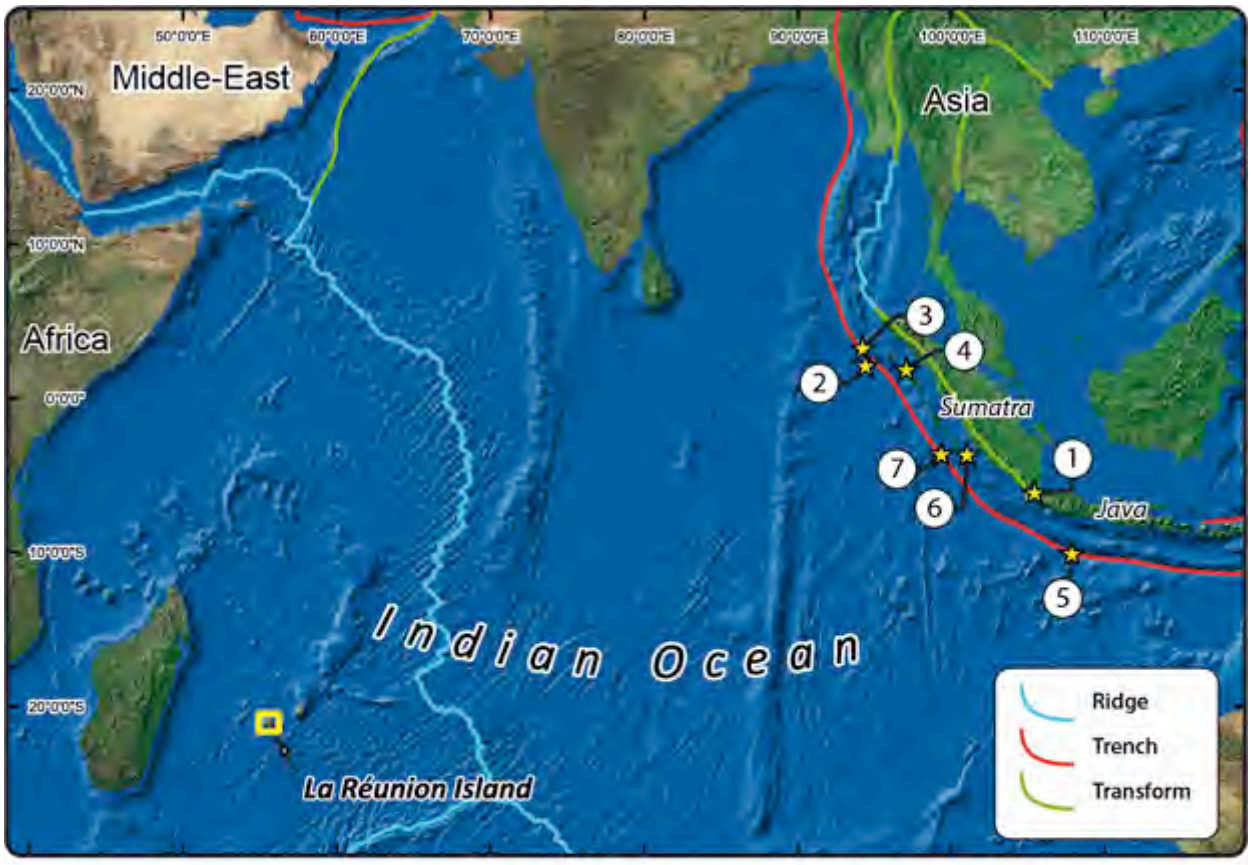

	Date	Mw or Ms	Depth (km)	Ditance (km)	Observed TTT	Max runup (m)	Loc Max runup
①	27/08/1883	Vol.		5620	7h39	7	Saint-Paul
②	04/01/1907	7.8	30 ¤	4950	7h29	~2	Saint-Pierre
③	26/12/2004	9.0	30	4990	6h55	2.74*	Port Est
④	28/03/2005	8.6	30	5170	8h10	?	Sainte-Marie
⑤	17/07/2006	7.7	34	5700	8h26	0.51	Saint-Leu
⑥	12/09/2007	8.5	34	5260	7h20	?	Sainte-Marie
⑦	25/10/2010	7.8	20.6	5100	7h20	1.72	Sainte-Marie

Figure 1. Location of the sources and local effects of tsunamis that affected La Réunion Island since 1883 (in italics when uncertain; Sources: plates boundaries from Coffin et al. (1998); ¤: Kanamori et al. (2010); *: Okal et al. (2006); background ESRI).

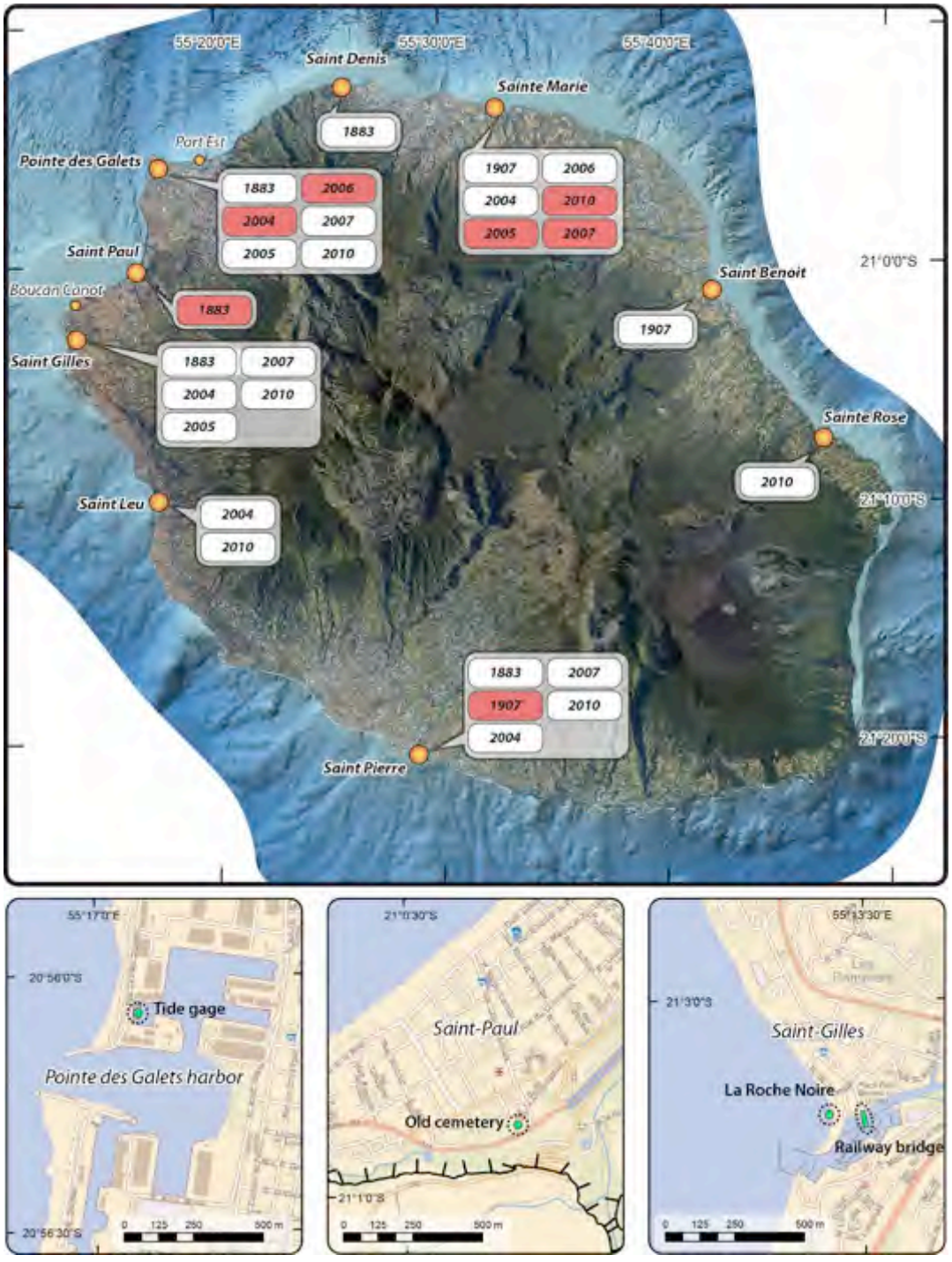

Figure 2. Synthesis of local effects of tsunamis of transoceanic origins (in red the most affected place for each tsunami) and locations mentioned in the text (background data from IGN, SHOM and DDE).

1.1. August 27th, 1883 Tsunami

On August 27th, 1883, at 9:58 LT in Indonesia (UTC+7:07:12), the explosion of the Krakatau volcano (Indonesia) triggered a tsunami with waves reaching 30 meters high and runup up to 40m along the Sundra Strait, killing 36,000 people (Choi et al. 2003; van Den Bergh et al. 2003; Pelinovsky et al. 2005). Its impact was felt in the Indian Ocean, including the Seychelles Islands (0.3m runup), Mauritius (0.8m) and Rodrigues Island (1.8m) (Choi et al. 2003; Dunbar 2010).

In La Reunion Island, the newspaper *Le Créole de l'Île de la Réunion* of August 29th, 1883 records the observation of a several feet high tidal bore in Saint-Denis on August 27th, entering the Barachois river for a few minutes. This was followed by a recession with a "brutal" current, carrying boats away despite chains and anchors. The whole water movement occurred several times, emptying the basin and drying the surrounding beaches during withdrawal. The September 2nd, 1883 issue of the newspaper *La Malle,* reported impacts in other places, and evaluation of a greater impact on the southern part of the island's west coast. At the Pointe des Galets cape, the sea "rose violently"; in Saint-Gilles. The sea reached the still-existing railway, with a runup value of 3.5m; the sea level variation was even more intense in Saint-Pierre where it started at 11 with a bore and ended around midnight. In Saint-Pierre, the harbor front basin was filled and emptied twice every 10 minutes with currents characterized as "strong". In Saint-Paul, "the sea rose just as quickly, flooding the whole town and even, carrying graves and coffins away from the old cemetery". According to the newspaper *le Journal de l'île de la Réunion* dated August 28th, 1883, "the phenomenon reached the cliffs leaving great amounts of sand". This old cemetery is located at the Rosalie Javouhey church, 630m inland, at a 7m altitude. Unfortunately, the resulting deposits were not found during the field investigations.

The same phenomenon was observed as starting at 11 LT on August 27th, in Saint-Pierre. In 1883, La Réunion's local time corresponded to UTC+3:41:52. The sea disturbance was first observed and timed at approximately 7:18 UTC on the 27th (T_0+4h16). The propagation models estimate the corresponding tsunami travel time from the Krakatau volcano to La Réunion Island to be around 7h45 (TsuDig, NGDC). It seems impossible that the tsunami that reached La Reunion Island could have been triggered during the paroxysmal phases of the eruption of Krakatao (9:58 LT, third blast), even if some sea level disturbances were triggered atmospherically by the explosion (Garrett 1970). A more accurate estimation of the time the tsunami initiated would correspond to 6:30 Indonesian time (LT). This corresponds to the 6:36 LT Krakatau's second blast, collapse of the Danan peak and formation of its caldera (Choi et al. 2003). Considering the 6:36 LT blast as the one responsible for triggering the tsunami that struck La Reunion Island, an arrival at **T_0+7h39** can be estimated. However, it is noteworthy that the major effects felt in Saint-Paul started at 15:00 LT in La Réunion, which is more in accordance with the Indian Ocean tide gauge records (Choi et al. 2003).

1.2. January 4th, 1907 Tsunami

On January 4th, 1907, at 5:19 UTC (Dunbar 2010), a magnitude Ms=7.8 earthquake occurred close to the location of the December 26th, 2004 tsunami source (Kanamori et al. 2010), triggering a tsunami

which hit Indonesia and Sri Lanka. Around 16:30 LT, workers in Saint-Pierre's harbor basin gave the alert, observing a 2m rise in water level. The water surged into the harbor channel and gently flooded the harbor banks. The seawater disturbance was still observed on the evening of January 4th (newspaper *Le Journal de l'Île de La Réunion,* dated January 8th).

In Saint-Benoit, at the same time – i.e. 16:30 LT – the sea quickly receded 100m "behind the capes of St Benoit's reef" without seeming rough. Some witnesses rushed to the cleared sea floor to pick up fish, but soon abandoned their catch: the sea level rose back, flooding inland over the highest tide limits. Several similar cycles were observed until 21:00 LT when the sea level went back to normal (*Le Journal de l'Île de La Réunion* dated January 8th).

La Patrie Créole newspaper, dated January 8th, confirms these observations. It also adds the record of a sea withdrawal in Sainte-Marie that exposed rocks that are never visible, even at the lowest tides.
In 1907, LT in La Reunion Island was still UTC+3:41:52. So it was 12:48 UTC at the beginning of the observations, which corresponds to an arrival at **T_0+7h29** after the earthquake.

1.3. December 26th, 2004 Tsunami

On December 26th, 2004, at 00:58 UTC, a magnitude Mw=9.0 earthquake triggered a tsunami which impacted most countries bordering the Indian Ocean, killing 227.898 people (Dunbar 2010).
Shortly after the December 2004 disaster, an International Tsunami Survey Team (ITST) was sent to La Reunion Island. The results of the field survey (Okal et al. 2006) show that the whole island was impacted, with a maximal effect on the northwestern coast between Pointe des Galets and Saint-Gilles. Maximal runup values were recorded at the La Roche Noire beach - which is not protected by a coral reef - reaching 2.44m high and in the basin of the Pointe des Galets harbor reaching 2.74m (Okal et al. 2006). Seventeen boats sank at Sainte-Marie harbor, located on the northern shore of the Island (Figure 2).

Additional results from the PREPARTOI program allowed to gather original testimonies indicating a sea level recession of 1.8m in Saint-Gilles, followed by a 1.78m runup, equivalent to a "very fast tide". Seven motorboats sank. In Sainte-Marie, 11 motorboats sank. At La Roche Noire beach (Saint-Gilles), according to the lifeguards, one could walk to the entrance of the harbor, which confirms the previously mentioned 1.8m sea level drop. In Port Réunion, a public harbor located inside the Pointe des Galets basin, the staff observed a 1m high tidal wave entering the basin. It was followed by a 10-min period recession and elevation of sea level. In Port Est harbor, the 12 moorings of a 40,000t container ship (MSC "Uruguay") were broken by the sea disturbances at 15:30 LT. The Pointe des Galets tide gauge recorded the arrival of the tsunami at 11:55 LT (7:55 UTC), corresponding to **T_0+6h55**. The sea level disturbance was recorded until the morning of December 28th.

1.4. March 28th, 2005 Tsunami

On March 28th, 2005, at 16:09 UTC, a magnitude Mw=8.6 earthquake was recorded in the same area as those of 1907 and 2004, also triggering a tsunami. "A 3m tsunami damaged the port and airport on

Simeulue" (ITIC 2005). According to ITIC, the maximal recorded runup reached 2m on the west coast of Nias Island (located off Sumatra's coast).

At La Reunion Island, in the night of the 28-29th, at 5:00 LT a 0.4m sea level elevation was recorded in Saint-Gilles' harbor. The sea level disturbance lasted until 6:30 LT. In Sainte-Marie, the harbor staff observed a similar phenomenon reaching 0.2 to 0.3m higher than the highest tides. The staff recorded the occurrences of small eddies and wrinkles. The water looked particularly turbid (*Le Journal de l'Île de La Réunion* dated March 30th, 2005). The Pointe des Galets tide gauge recorded the sea level disturbance from 4:20 to 9:00 LT, that is from 0:20 to 5:00 UTC (**T_0+8h10**)

1.5. July 17th, 2006 Tsunami

On July 17th, 2006, at 8:19 UTC, a magnitude Mw=7.7 earthquake (USGS) was recorded off Java Island, triggering a tsunami which devastated Java's southern coast (Lavigne et al. 2007).
At La Reunion Island the Pointe des Galets tide gauge recorded the tsunami from 20:45 LT on the 17th to 19:00 LT on the 18th. It corresponds to an arrival at 16:45 UTC, **T_0+8h26**. A listener of Radio FreeDom (popular local radio station) called the radio station to report having observed unusual waves in Sainte-Marie harbor at 23:00 LT (*Le Journal de l'Île de La Réunion* dated July 19th).
An 0.8m sea level rise was observed in Pointe des Galets harbor, with "strong currents", as well as in Saint-Pierre harbor. At the Port Est commercial harbor, at 6:30 LT on the 18th, the sea disturbances broke the moorings of the MSC "Napoli", a 62,000t capacity bulk carrier. Additionally, a 0.51m runup was measured in Saint-Leu.

1.6. September 12th, 2007 Tsunami.

On September 12th, 2007, at 11:10 UTC, a magnitude Mw=8.5 earthquake was recorded off Sumatra's coasts. At La Reunion Island, a rapid 0.3-0.4m sea level rise was observed in Saint-Gilles harbor at 22:45 LT. It was followed by a 0.2m recession and the disturbances repeated every 5-10 minutes. Very strong currents were observed. On that particular day, the tides were of a very low level, limiting the flood to a 1.13m altitude. Around 23:00 LT (19:00 UTC), the authorities recorded an unusual sea level elevation of 0.6m in Sainte-Marie harbor. It took the sea 2min to rise and 1min to recede, after a 2min transition. This alternation continued for 1h30. At the Pointe des Galets harbor, a 0.20-0.30m amplitude oscillation was observed. The tide gauge recorded a 0.24m amplitude oscillation at 22:30 LT (18:30 UTC, **T_0+7h20**). In Port Est, no effect was noticed. All boats had already been taken out of the harbor.

1.7. October 25th, 2010 Tsunami

On October 25th, 2010, a magnitude Mw=7.8 earthquake was recorded at 14:42 UTC in the Kepulauan Mentawai archipelago, in Indonesia. At La Reunion Island, the Pointe des Galets tide gauge recorded the tsunami from 22:00 UTC on the 25th to 19:00 UTC on the 26th (**T_0+7h20**).
A specific article was recently accepted by two of this article's authors about the October 25th event (Sahal and Morin accepted), describing its effects and how the authorities managed the crisis. The maximal measured runup reached 1.72m in Sainte-Marie harbor, sinking 4 motorboats.

Figure 3. Video footage extracts of the March 20th, 2010 wave train observed at Boucan-Canot. A: arrival of the wave train, B: flood, C: back to normal. Courtesy M. Ropert.

2. DISCUSSION

Precision of measured runup values depends entirely on the quality and reliability of information sources. The older an event is, the lower the quality of the information describing it is. Recent events are described by crosschecking various witnesses' records, while events prior to 2004 (1907 and 1883 events) are described accordingly to a single source, that is old newspapers. A probability exists for the occurrence of tsunami triggered locally from La Réunion island's flanks. Kelfoun et al. (2010), who recently modeled potential local sources that could affect La Réunion show important potential impacts for such sources. On March 20th, 2010, the OVPF-IPGP network recorded two low magnitude earthquakes on La Reunion Island. The first one occurred at 13:19 LT and was followed by the second – of a higher magnitude - at 14:43 LT. Their location, out of the sensors network, is estimated to be west of the island. A few minutes later, a series of 3 unexpected waves flooded the beaches of Boucan-Canot and La Roche Noire. These two beaches of the west coast are located 3km apart and are unprotected by a coral reef barrier. The lifeguards were "surprised" by this unusual phenomenon. Their offices, respectively 5 and 3m above the lowest tides in Boucan-Canot and the La Roche Noire beach were flooded. A maximal runup of 5.7m was measured in Boucan-Canot, where several people were injured when projected onto rocks. Others were taken out to sea by the reflux and needed boat rescue. A witness in Boucan-Canot filmed the arrival of the wave train and the consecutive flood (Fig 3). The study and time calibration of the video footage reveal an arrival at 15:08 LT (**T_0+0h25** after the second earthquake). The seismographs of the OVPF-IPGP network did not record a signal indicating a submarine landslide.

The March 20th, 2010 event was neither covered by the media, nor noticed by the authorities. Only the beach surveillance services noticed the phenomenon and its consequences on swimmers. No certainty exists concerning the origins of this inundation (ground swells, unusually large swells or tsunami of a local origin?). The person who filmed the event also filmed surfers at the same place a few hours before the arrival of the "unusual" wave train. After studying both films, one noticed that on this day, the waves displayed an entirely different comportment than that of the flooding wave train.
Considering that this March 20th event was identified through word-of-mouth and not through official

or media means, one could suppose that similar event may have occurred in the past without being referenced. Also, potential regional sources of tsunamis (Madagascar, the Karthala volcano, etc.) are not represented in this catalog as no event of such origin was identified (Hartnady 2005a; Hartnady 2005b).

Concerning the 1883 Krakatau tsunami, the maximal runup measure is not in accordance with the ones measured in the rest of the Indian Ocean (Choi et al. 2003; Pelinovsky et al. 2005). Nevertheless, considering: (1) the number of newspapers referring to this event; (2) the precision of observations and their spatial distribution; (3) the fact that August is out of the cyclonic season; (4) the observed sea level recede; (5) and the fact that the only documented quantified effects in the Indian Ocean were based solely on tide gauge records (that often underestimate the coastal impact); the effects of the 1883 Krakatau tsunami can be considered as accurate in La Réunion Island.

A newspaper article recalls several inhabitants' memory of a past tsunami occurrence: the 1883 tsunami was "a violent tidal wave that looked just like the one observed in 1867, when the Peruvian earthquake occurred" (*La Malle*, dated October 25th, 1883). Such information raises several questions: could this be the August 13th, 1868 earthquake (Mw=8.5) and associated tsunami affecting La Réunion? Could a tsunami triggered in Peru or Chile have an impact in the western Indian Ocean, or is the journalist recalling effects observed in Peru? The 1868 tsunami had a maximal runup of 18m in Arica (Chile) and only reached 1.2m high in Sydney, the most western measured runup for this tsunami (Soloviev and Go 1974).

Due to lack of available archives, impact evidence could neither be found for the tsunami triggered by the November 24th, 1833 Indonesian earthquake (Mw=8.8-9.2, Zachariasen et al. 1999), nor for the February 16th, 1861 Indonesian one (Ms=8.5, Dunbar 2010), nor for the November 27th, 1945 Makran event (Ms=8.0, Rastogi and Jaiswal 2006; Mokhtari et al. 2008; Heidarzadeh et al. 2009).

The December 2004 event is the only one for which a regional field survey was conducted in the vicinity of La Réunion Island (Obura 2006; Okal et al. 2006). Therefore, very little information was available in the literature about the effects the tsunamis had in the region. Only tide gauge records are usually considered for mapping and studying far field tsunami effects. Field surveys and archive research appear to be of major importance in studying local tsunami amplification and effects. The PREPARTOI program will soon provide far field high resolution modeling of the shoaling effects along La Réunion Island's coasts using different tsunami sources, which will help the understanding of such phenomenon.

3. CONCLUSIONS

This first catalog of tsunamis that historically impacted La Réunion Island mainly shows teletsunamis that affected other countries of the Indian Ocean. All their sources are located on the Indonesian margin, which does not mean tsunamis from the Makran region would not affect La Réunion Island. It is essentially the west coast of the island which suffers the most important impacts, probably due to a

"wrap around" phenomenon and an amplification at the opposite coast, as previously demonstrated by Hébert et al. (2007).

The observed travel times of the tsunamis triggered on the Indonesian margin range from 6h55 to 8h26 post earthquake, according to the witness records gathered. This amount of time, although reasonable for a response by the authorities, was not always enough to respond adequately to a tsunami threat (Sahal and Morin accepted). This response should improve from now on, thanks to the recent revision of the local alert and responses procedures. Finally, one must note that the Pointe des Galets tide gauge is not appropriately located in its harbor; it is in a protected basin, and always underestimates the impacts on the other harbors (Table 2). Relocating this tide gauge in its basin and implanting new tide gauges in Sainte-Marie and Saint-Pierre harbors would considerably improve the quantification of future tsunamis, for the benefit of La Réunion Island as well as other Indian Ocean countries.

Table 2. Maximal amplitudes during the identified tsunamis since 2004 as recorded by the Pointe des Galets tide gauge (located on Figure 2) and measured runup values (all in meters).

Tsunami event	***Maximal amplitude recorded by the tide gauge (crest-to-trough)***	***Maximal runup measured on the island***
26/12/2004	0.72	2.74
28/03/2005	0.19	*?*
17/07/2006	0.24	0.51
12/09/2007	0.24	*?*
25/10/2010	0.39	1.72

Acknowledgments

The PREPARTOI Program is founded by the MAIF Foundation. Many thanks to the Prefecture of La Réunion for supporting the program and to the local archives services of La Réunion Island (Archives Départementales) for allowing access to non-communicable archives. Thanks to Karl Hoarau (Université de Cergy-Pontoise) for his precious advice and expertise on cyclones in La Réunion Island.Thanks to M. Ropert for allowing us to use his video of the March 20th, 2010 event.
Thanks to Marion Cole for her review of the English version of this article.

REFERENCES

Choi, B H, E Pelinovsky, K O Kim and J S Lee (2003) Simulation of the trans-oceanic tsunami propagation due to the 1883 Krakatau volcanic eruption. Natural Hazards and Earth System Science 3 321-332.

Coffin, M F, L M Gahagan and L A Lawver (1998) Present-day Plate Boundary Digital Data Compilation, Technical Report No. 174. Austin, TX, USA: 5.

Dunbar, P. (2010) "NOAA/WDC Historical Tsunami Database." from http://www.ngdc.noaa.gov/hazard/tsu.shtml.

Garrett, C J R (1970) A theory of the Krakatoa tide gauge disturbances. Tellus 22 (1):43-52.

Hartnady, C (2005a) Continental slope landslide- and oceanic island volcano-related tsunami potential in the Western Indian Ocean. East African Rift 2005, Mbeya, Tanzania.

Hartnady, C (2005b) De la possibilité d'apparition de tsunamis sur la côte est-africaine et les îles de l'Océan indien. La prévention des catastrophes en Afrique - SIPC Informations 27-30.

Hébert, H, A Sladen and F Schindelé (2007) Numerical Modeling of the Great 2004 Indian Ocean Tsunami: Focus on the Mascarene Islands. Bulletin of the Seismological Society of America 97 S208-S222.

Heidarzadeh, M, M Pirooz, N Zaker and A Yalciner (2009) Preliminary estimation of the tsunami hazards associated with the Makran subduction zone at the northwestern Indian Ocean. Natural Hazards 48 (2):229-243.

Itic (2005) Tsunami Newsletter. XXXVII (2):3-4.

Kanamori, H, L Rivera and W H K Lee (2010) Historical seismograms for unravelling a mysterious earthquake: The 1907 Sumatra Earthquake. Geophysical Journal International 183 (1):358-374.

Kelfoun, K, T Giachetti and P Labazuy (2010) Landslide-generated tsunamis at Réunion Island. Journal of Geophysical Research 115 1-17.

Lavigne, F, C Gomez, M Giffo, P Wassmer, C Hoebreck, D Mardiatno, J Priyono and R Paris (2007) Field observations of the 17th July 2006 Tsunami in Java. Natural Hazard & Earth Sciences Systems 7 177-183.

Mokhtari, M, I Abdollahie Fard and K Hessami (2008) Structural elements of the Makran region, Oman sea and their potential relevance to tsunamigenisis. Natural Hazards 47 (2):185-199.

Obura, D (2006) Impacts of the 26 December 2004 tsunami in Eastern Africa. Ocean & Coastal Management 49 (11):873-888.

Okal, E A, A Sladen and E Okal (2006) Rodrigues, Mauritius, and Réunion Islands Field Survey after the December 2004 Indian Ocean Tsunami. Earthquake Spectra 22 S241.

Pelinovsky, E, B H Choi, A Stromkov, I Didenkulova and H-S Kim (2005) Analysis of tide-gauge records of the 1883 Krakatau tsunami. Tsunamis: Case Studies and Recent Developments. K. Satake**:** 57-78.

Rastogi, B K and R K Jaiswal (2006) A catalog of tsunamis in the Indian Ocean. Science of Tsunami Hazards 25 (3):128-143.

Sahal, A and J Morin (accepted) Effects of the October 25th, 2010 Mentawai Tsunami in La Réunion Island (France): Observations and Crisis Management. Natural Hazards.

Sahal, A, B Pelletier, J Chatelier, F Lavigne and F Schindelé (2010) A catalog of tsunamis in New Caledonia from 28 March 1875 to 30 September 2009. C. R. Geoscience 342 434-447.

Soloviev, S L and C N Go (1974) A catalogue of tsunamis on the western shore of the Pacific Ocean. Moscow, Academy of Sciences of the USSR, Nauka Publishing House.

Van Den Bergh, G D, W Boer, H De Haas, T Van Weering and R Van Wijhe (2003) Shallow marine tsunami deposits in Teluk Banten (NW Java, Indonesia), generated by the 1883 Krakatau eruption. Marine Geology 197 13-34.

Zachariasen, J, K Sieh, F W Taylor, R L Edwards and W S Hantoro (1999) Submergence and uplift associated with the giant 1833 Sumatran subduction earthquake: Evidence from coral microatolls. Journal of Geophysical Research 104 (B1):895-919.

ISSN 8755-6839

SCIENCE OF TSUNAMI HAZARDS

Journal of Tsunami Society International

Volume 30 Number 3 2011

DETECTION OF LOCAL SITE CONDITIONS INFLUENCING EARTHQUAKE SHOCK AND SECONDARY EFFECTS IN THE VALPARAISO AREA IN CENTRAL-CHILE USING REMOTE SENSING AND GIS METHODS

Barbara Theilen-Willige [1] **and Felipe Barrios Burnett** 2

[1] TU Berlin, Institute of Applied Geosciences, Berlin, Germany, E-mail: Barbara. Theilen-Willige@t-online.de

[2] Hydrographic and Oceanographic Service of the Chilean Navy, Department of Hydrography, and E-mail: fbarrios@shoa.cl

ABSTRACT

The potential contribution of remote sensing and GIS techniques to earthquake hazard analysis was investigated in Valparaiso in Chile in order to improve the systematic, standardized inventory of those areas that are more susceptible to earthquake ground motions or to earthquake related secondary effects such as landslides, liquefaction, soil amplifications, compaction or even tsunami-waves. Geophysical, topographical, geological data and satellite images were collected, processed, and integrated into a spatial database using Geoinformation Systems (GIS) and image processing techniques. The GIS integrated evaluation of satellite imageries, of digital topographic data and of various open-source geodata can contribute to the acquisition of those specific tectonic, geomorphologic/ topographic settings influencing local site conditions in Valparaiso, Chile. Using the weighted overlay techniques in GIS, susceptibility maps were produced indicating areas, where causal factors influencing near-surface earthquake shock occur aggregated. Causal factors (such as unconsolidated sedimentary layers within a basin's topography, higher groundwater tables, etc.) summarizing and interfering each other, rise the susceptibility of soil amplification and of earthquake related secondary effects. This approach was used as well to create a tsunami flooding susceptibility map. LANDSAT Thermal Band 6-imageries were analysed to get information of surface water currents in this area.

Key Words: *Local site conditions, tsunami and slope failure susceptibility, Central-Chile, remote sensing and GIS*

Science of Tsunami Hazards, Vol. 30, No. 3, page 191 (2011)

1. INTRODUCTION

The Chilean subduction zone has one of the highest levels of seismic activity in the world. Large mega-earthquakes of magnitudes >8 occur on the average every 5–10 years (Table 1). These earthquakes result from the on-going active subduction of the Nazca plate beneath South America (Vigny et al., 2009). Preparing for such mega-earthquakes requires a long-term public policy in enforcing building regulations (Madariaga et al., 2010). When planning and rebuilding in earthquake prone areas, local site conditions that influence earthquake ground motions need to be carefully evaluated. For earthquake disaster preparedness, it is helpful to know which areas might be more susceptible to ground motions and secondary effects and distinguish them from areas affected by specifically by local site conditions.

Table 1. Earthquakes with Magnitudes >7 according to Winckler-Grez & Vásquez-Álvarez (2008) and USGS (2010)

Year	Length (km)	Width (km)	Displacement (m)	Ml
1575				7.0 – 7.5
1647	365			8.5
1730	350 – 550	100-150	6 - 8	8.75
1822	200 – 330	100-150	3 - 6	8.5
1906	365 – 330	100-150	3 - 6	8.2 – 8.3
1985	170	100	1.23 – 2.80	7.8
2010	550	100	3 - 4	8.8

Local geologic conditions are the cause of differences in earthquake intensity. However, particular conditions of specific areas and the degree to which are they affected by the earthquake's ground motions are often the main cause of intensity variations.
Earthquake ground motions depend primarily on such factors as the quake's magnitude, the physical properties of the strata along the rupture zone, the distance from the fault and the local geologic conditions. The most intense shaking generally occurs near the rupturing fault area and decreases with distance. However, the ground motions at one site can be stronger than at another site, regardless of the distance (Gupta, 2003).

The variability in earthquake-induced damage is mainly determined by the local lithologic and hydro-geological conditions. These conditions, in turn influence the amplitude, the frequency and duration of ground motion at a site. Flat areas (below 10° slope gradient) within morphologic basins and depressions are usually covered by younger, unconsolidated sediments. Ground with high liquefaction or compaction response is occurs in areas with newly formed sediments. Soft soils can amplify shear waves and, thus, amplify ground shaking. Unconsolidated sediments slow the earthquake wave velocity, trapping the energy and thus causing more intense shaking. Newer sediments near a source of water often contain water-filled pore spaces. As earthquake's energy cyclically compresses these sediments, the pore pressure in the pore spaces

increases to a level greater than the confining pressure of the soils above them, causing small geyser-like sand boils that spew water and sand and result in ground subsidence. If buildings and other structures sit atop these hazardous areas, they have a higher risk of damage or collapse.

The fundamental phenomenon responsible for the amplification of motion over soft sediments is the trapping of seismic waves due to the impedance contrast between sediments and underlying bedrock. When the structure is horizontally layered, this trapping affects body waves, which travel up and down in the surface layers. When lateral heterogeneities are present (such as thickness variations in sediment-filled valleys), this trapping also affects the surface waves, which develop on these heterogeneities. The interferences between these trapped waves lead to resonance patterns, the shape and the frequency of which are related with the geometrical and mechanical characteristics of the structure (Ehret & Hannich, 2004).

Groundwater level variations and associated saturation changes in sand layers within near-surface aquifers can influence local response spectra of the ground motion, through modification of shear-wave velocity. Wetlands generally have a higher damage potential during earthquakes due to longer and higher vibrations. Recently formed sediments will slow the velocity of the earthquake waves, trapping the energy and causing large amplitudes of shaking. Older compacted materials that over time have densified or transitioned from sand to sandstone and cemented together are less responsive for example to liquefaction. Changes of the groundwater level can have a considerable influence upon the liquefaction potential of a region due to in-situ pore-water pressure responses in aquifers during earthquakes triggering mechanism of liquefaction (Hannich et al., 2006). Liquefaction that affects the human-built environments is mostly limited to the upper 15 meters of soil.

Due to seasonal and climatic reasons a stronger earthquake during a wet season will probably cause more secondary effects than during a dry season. In very hot and dry seasons the risk of liquefaction or landslides is generally lower than in spring times. These seasonal effects should be monitored systematically.

Earthquakes cause damage to buildings and other structures both in near and far fields. This phenomenon of far field damages to buildings has been reported, worldwide, notable being the 1985 Mexico earthquake, where the epicenter was 400 km offshore from the Mexico city, which suffered very heavy damage (Steinwachs, 1988). This observation emphasizes the importance of local site conditions in either reducing or enhancing the earthquake hazard in a region.

Maps of seismic site conditions on regional scales require substantial investment in geological and geotechnical data acquisition and interpretation. Macroseismic maps that can help to detect local site conditions in Chile are based on different standards and scales (Ceresis, 1985). There is a strong need to improve the systematic, standardized inventory of areas that are more susceptible to earthquake ground motions or to earthquake related secondary effects such as landslides, liquefaction, soil amplifications, compaction or tsunami-waves. Therefore a uniform data base with a common set of strategies, standards and formats should be implemented.

Topographic variations can be considered as an indicator of near-surface lithology to the first order; with steep mountains indicating rock, nearly flat basins indicating soil, and a transition between the end members on intermediate slopes. In the seismically active region of Haiti, information about surficial geology and shear-wave velocity (*V*S) either varies in quality, varies spatially, or is not accessible. The similarity between the topography and the surficial site condition map, derived from geology is striking. Therefore the service provided by the USGS providing V_s^{30} data from all over the earth's surface based on these correlations (Wald & Trevor, 2007, USGS Seismic Hazard Program, Global V_s^{30} Map Server) was used for these investigations in Central-Chile.

1.2. Aim of study

The main objective of this study is to investigate the potential contribution of remote sensing and GIS techniques for the detection of areas more susceptible to earthquake ground motions due to local site conditions. The evaluation of satellite imageries and of digital topographic data is of great importance since it contributes to the acquisition of the specific geomorphologic/topographic settings of earthquake hazard affected areas by extracting geomorphometric parameters based on Digital Elevation Model (DEM) data. As digital elevation data acquired by SRTM (Shuttle Radar Topography Mission, 90m spatial resolution) and ASTER-data (30 m resolution, interpolated up to 15 m) are readily and freely available, so the standardized approach described in this paper can be utilized worldwide.

2. GEOLOGIC, SEISMOTECTONIC AND GEOMORPHOLOGIC SETTING

The study area along Central Chile is a segment of one of the longest coherent subduction zones known worldwide. This convergent plate margin has been created by the collision of the oceanic Nazca plate with the continental South American plate. The main characteristic features generated by the conversion are the deep-sea trench (having a maximum depth of 8000 m along the west front of the study area), the Wadati Benioff Zone (WBZ) and the impressive Andean orogen. The shallow part of the WBZ - which hosts the seismogenic zone - has a dip angle of approximately 20◦ (Sobiesiak, 2004). The Nazca plate moves towards the South American plate at a rate of about 7 cm/year. Along this fault zone, the Nazca plate dives into the earth's mantle. Because of the rapid convergence, the Chilean subduction has strong seismic activity, with earthquakes of magnitude 8 occurring every decade on the average. One earthquake of M > 8.7 occurs at least every century. In addition, the largest earthquake ever recorded in recorded history (Mw 9.4-9.5) occurred in 1960, just south of Concepcion in Central Chile (Vigny, 2010). Fig.1 shows earthquake epicenters and documented tsunami events in Central Chile. Fig. 2 provides a LANDSAT 3D-overview of the geomorphologic setting, showing mountainous areas subdivided by elongated valleys, broader basins and coastal lowlands covered by unconsolidated, Quaternary sediments.

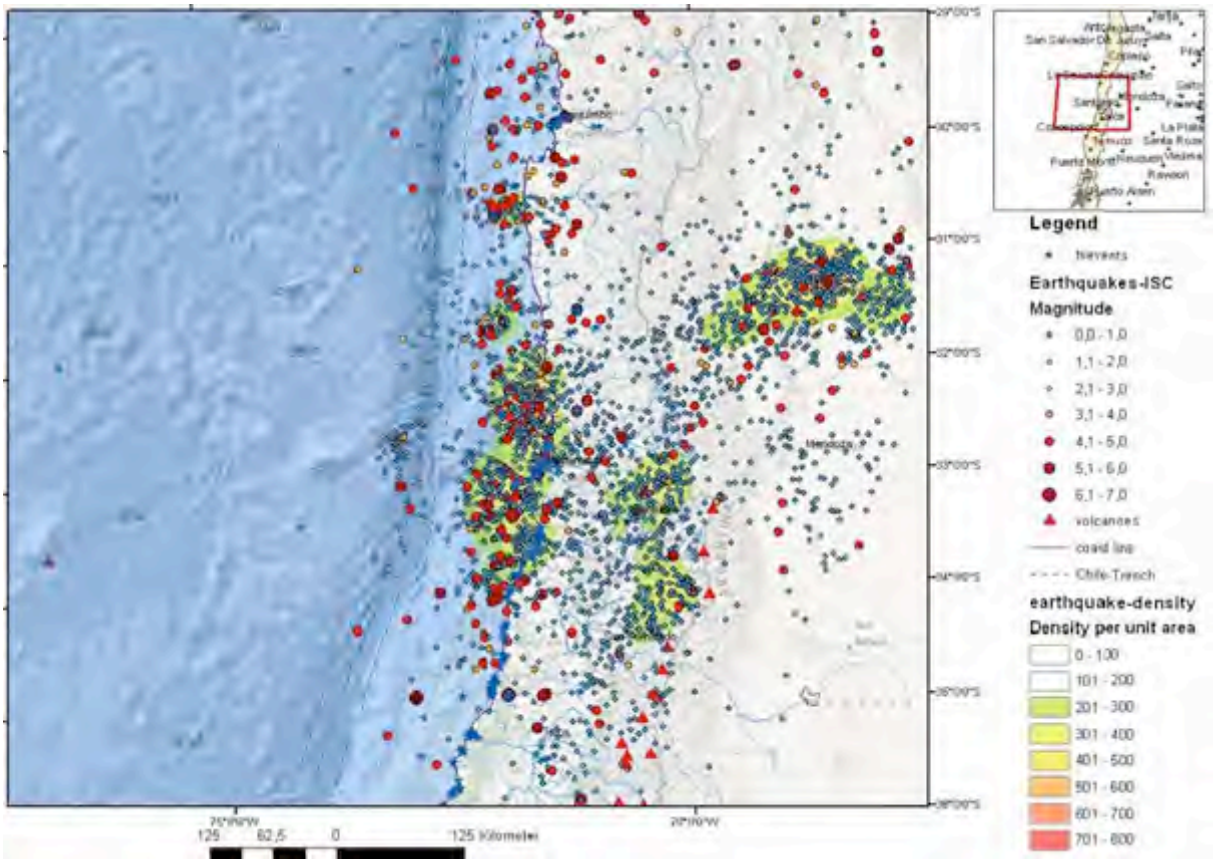

Fig.1. Earthquakes in Central-Chile (Earthquake data: USGS, ISC, NOAA, GFZ)

3. METHODS

GIS integrated geodata analysis can be used to detect, map and visualize factors that are known to be related to the occurrence of higher earthquake shock and / or earthquake induced secondary effects: factors such as lithology (loose sedimentary covers), basin and valley topography, fault zones or steeper slopes.

3.1. Evaluations of morphometric maps derived from Digital Elevation Data (DEM)

Morphometric maps such as slope, hillshade, height level, and curvature maps are generated based on SRTM and ASTER Digital Elevation Model (DEM) data using ArcGIS from ESRI and ENVI digital image processing software (ITT). Step by step factors can be extracted from these data that might be of importance for the detection of local site conditions. For example: The distribution of unconsolidated, youngest sedimentary covers can often be correlated with areas showing less than 10° slope gradient and no curvature (in the case of the curvature: negative curvatures represent concave,

zero curvature represent flat and positive curvatures represents convex landscapes). Height level maps help to search for topographic depressions covered by recently formed sediments, which are usually linked with higher groundwater tables. When extracting the lowest height levels of an area, it becomes visible where the areas with high ground-water tables can be expected (Fig. 3). When earthquakes occur such areas have often shown the highest damage intensities (Schneider, 2004).

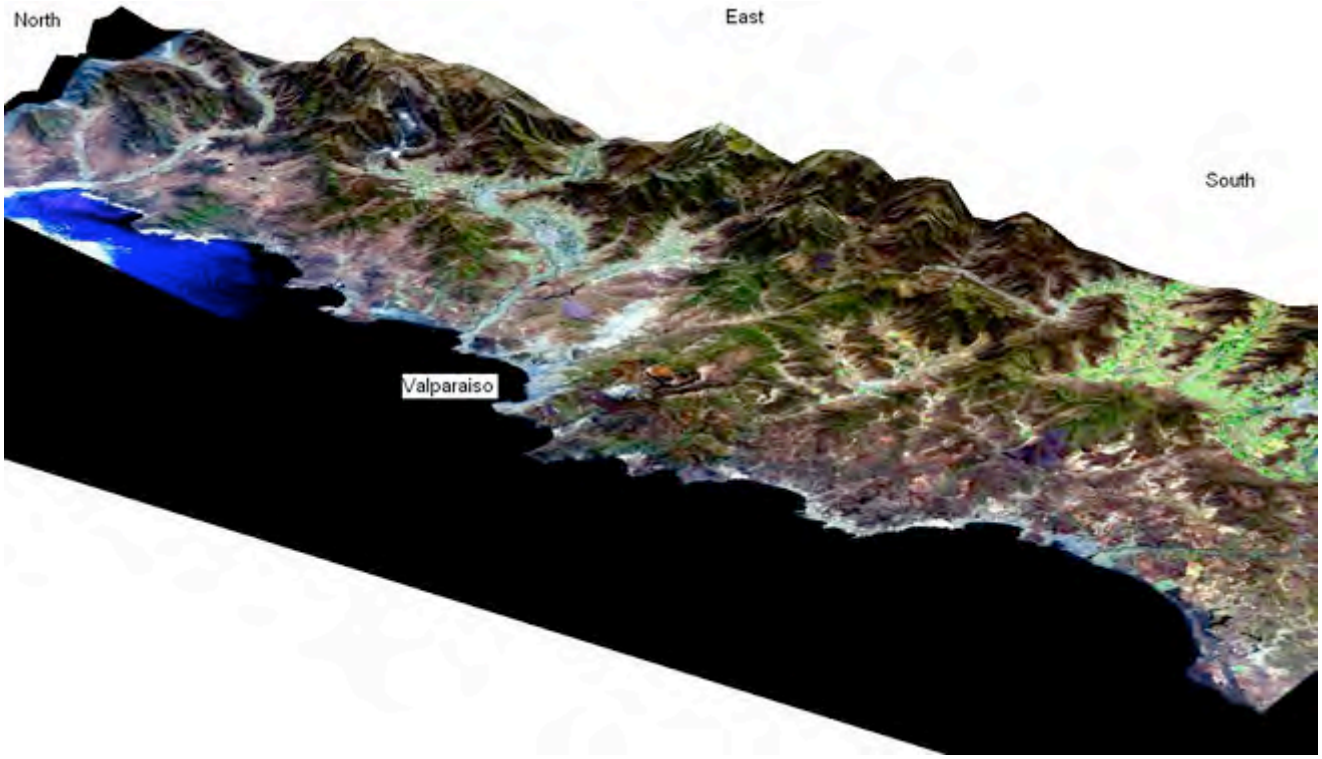

Fig. 2. Perspective 3D-view of a LANDSAT ETM image of the Valparaiso area merged with ASTER DEM data looking to the east

Slope gradient maps help detect areas where mass movements are likely to occur. Extracted from slope gradient maps are the areas with the steepest slopes and from curvature maps the areas with the highest curvature - as these are susceptible to landslides. Slopes with higher slope gradient (> 30°) are generally more susceptible to mass movements. By combining some of the causal or preparatory factors influencing earthquake shock intensity in a geo-referenced GIS environment, those areas can be detected where causal factors occur cumulatively and superimposed on each other. From SRTM and ASTER DEM data derived causal factors can be extracted such as:

- lowest *height levels* providing information of areas with relatively higher groundwater tables (here: 0-20 m),
- lowest *slope gradients* (< 5°-15°),

- lowest *minimum curvature or no curvature*, providing information of flat, broader valleys, basins and depressions with younger sedimentary covers and higher groundwater tables,
- highest *flow-accumulations,* providing information of areas with higher surface water-flow input, are combined with lithologic and seismo-tectonic information in a GIS data base as
- from geologic maps derived Quaternary sediment distributions and faults,
- from LANDSAT ETM imageries derived lineaments,
- from International Earthquake Centres downloaded earthquake data (International Seismological Centre, ISC, USGS, GFZ, etc.).

Causal or preparatory factors are extracted systematically in ESRI Grid-format. Of course, many further factors and data play an important role that - if available - should be included into the database.

The different factors are converted into ESRI-GRID-format and summarized/aggregated and weighted in % in the weighted overlay-tool of ArcGIS (Figs. 5 and 6) according their estimated influence on the local specific conditions or in equal percentages. Those areas are considered to be susceptible more to soil amplification of seismic waves where the following causal factors are summarizing and aggregating their effects: a) lowest height level of the terrain combined with relative high groundwater tables, b) flat morphology with low slope gradients and no curvature and c) loose sedimentary covers within a basin topography or within flat coastal areas. When an area is underlain by larger, active fault zones, especially when intersecting each other, the soil amplification susceptibility will probably rise, depending on given specific earthquake properties and parameters.

The percentage of influence of one factor is changing, as for example due to seasonal and climatic reasons, or distance to the earthquake source. As a stronger earthquake during a wet season will probably cause more secondary effects such as landslides or liquefaction than during a dry season, the percentage of its influence has to be adapted. Therefore the percentage of the weight of the different factors has to be adjusted as well to seasonal effects.

The sum over all factors / layers that can be included into GIS provides some information of the susceptibility in the amplification of seismic ground motions. After weightening (in %) the factors according to their probable influence on ground shaking susceptibility, maps can be elaborated, where those areas are considered as being more susceptible to higher earthquake shock intensities, where "negative" factors occur aggregated and interfering with each other. Whenever an earthquake occurs in these areas, now it can be derived better where the "islands" of higher ground shaking are most likely to occur by adding the specific information of the earthquake to the susceptibility map using the weighted overlay - approach.

The approach presented here is proposed to serve as a first basic data stock for getting a perception of potential sites susceptible to higher earthquake ground motions, followed by further integration of available data, such as movements along active faults, focal planes, shear wave velocities, uplift / subsidence estimates, 3D structure, lithologic properties, thickness of lithologic units, etc.

The analysis method and the integration rules can easily be modified in the open GIS architecture as soon as additional information becomes available. The database and maps thus obtained can facilitate and support the planning of additional geotechnical investigations. The more geotechnical site data exists, the better and more detailed the resulting susceptibility maps will be.

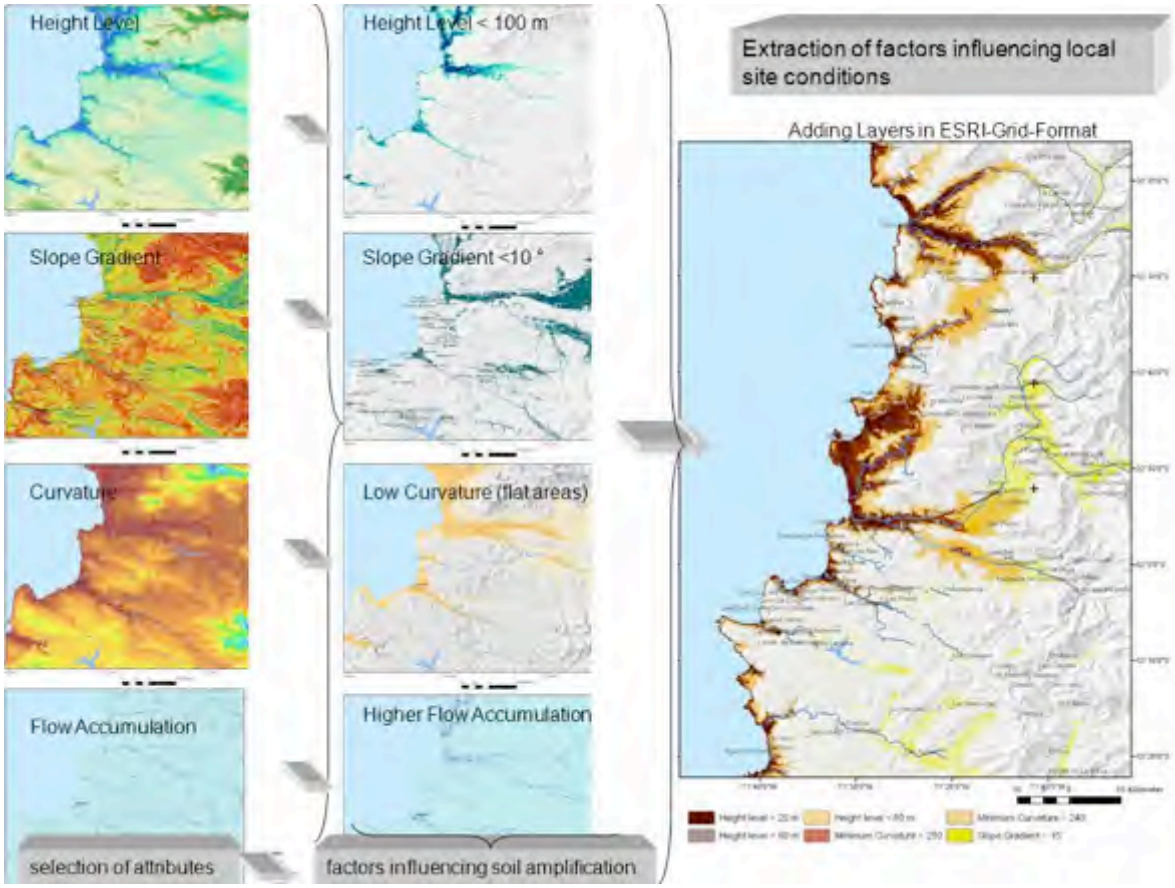

Fig. 3. Basic GIS approach for the extraction of causal factors influencing earthquake shock

3.2. Evaluations of LANDSAT Data

LANDSAT data were processed using various digital image processing methods using ENVI-Software / ITT. The main purpose of this image processing was to enhance the evaluation feasibilities for the detection of local site conditions and for structural analysis by integrating remote sensing and GIS technologies.

3.2.1. Lineament Analysis

Special attention was focussed on precise mapping of traces of faults (lineament analysis) on satellite imageries, predominantly on areas with distinct expressed lineaments, as well as on areas with intersecting/overlapping lineaments. Lineament analysis based on satellite imageries or DEM derived

morphometric maps can help delineate local surface-near fracture systems and faults that might influence seismic wave propagation and influence the intensity of seismic shock or might influence the susceptibility to secondary effects. Areas with intersecting, larger lineaments are probably exposed to relatively higher earthquake shock in case of stronger earthquakes. Linear arrangements of pixels depicting the same color/gray tone were mapped as linear features (the term lineament is a neutral term for all linear, rectilinear or slightly bended image elements). Lineaments often represent the surface expression of faults, fractures or lithologic discontinuities (Fig.4). Lineaments are expressed as scarps, linear valleys, narrow depressions, linear zones of abundant watering, drainage networks, peculiar vegetation, landscape and geologic anomalies. The use of such analysis results is based on the assumption that lineament systems in a satellite image are closely connected and respond to deformation scheme change which is caused by changes of the stress field in the earth's crust. Lineament analysis based on remote sensing data can contribute to the kinematic analysis of the investigation area as the distribution, orientation and density of lineaments constrain the orientation and relative magnitude of principal stress and help examine the geometry of deformation. Often however, the lineament pattern reflects overprinting of complex stress orientation representing changes in the orientation of principal stress over space and time. Lineament analysis can contribute to the detection of structural features that in the field might not be visible or can be mapped only based on time and cost-intensive field investigations.

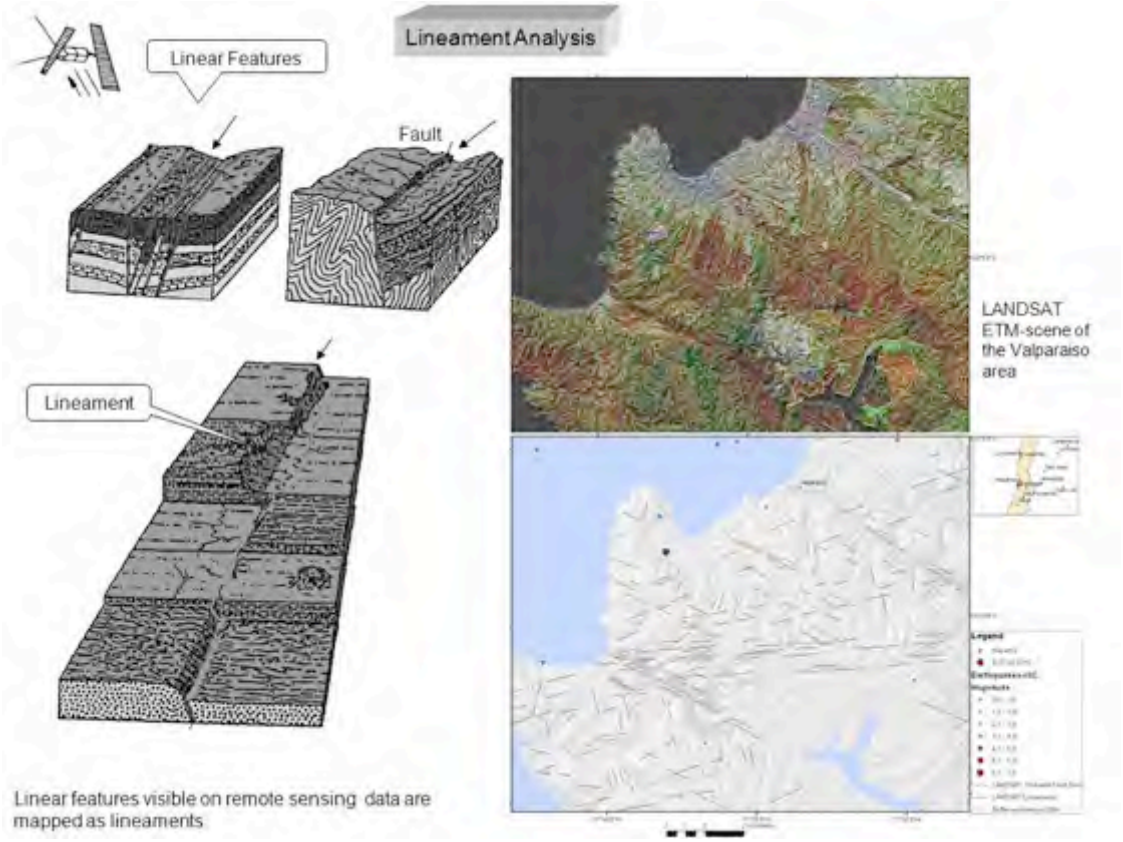

Fig. 4: Lineament analysis based on LANDSAT imageries

3.2.2. Deriving the Water Index (Normalized Difference Water Index – NDWI)

Groundwater table data are an important input when dealing with the seasonal influences on earthquake effects. A promising approach to obtain soil moisture variability is to use the greenness variations of biomass within an otherwise homogeneous canopy, because **variations in soil water directly affect the growth patterns of the overlying vegetation** (DeAlwis et al., 2007). For this purpose vegetation index (NDVI) and water index (NDWI) calculations were carried out (Fig. 5).
By considering information from both the LANDSAT 7 ETM+ Bands 4 and 5 an estimate of the soil moisture setting can be obtained. The Normalized Difference Water Index, NDWI, has been proposed to exploit this characteristic of Bands 4 and 5. The NDWI based on LANDSAT 7 ETM+ Bands 4 and 5 is defined as follows:

$$NDWI = \frac{(780-900\ nm) - (1550-1750)}{(780-900\ nm) + (155-1750)}$$

where (780−900 nm) is the reflectance in Band 4 of LANDSAT 7 ETM+ and (1550−1750 nm) is the reflectance in Band 5 of LANDSAT 7 ETM+. Of the seven bands available from the LANDSAT sensor, this methodology utilised two bands (2/5 and 4/5). The selection of these wavelengths maximises the reflectance properties of water.

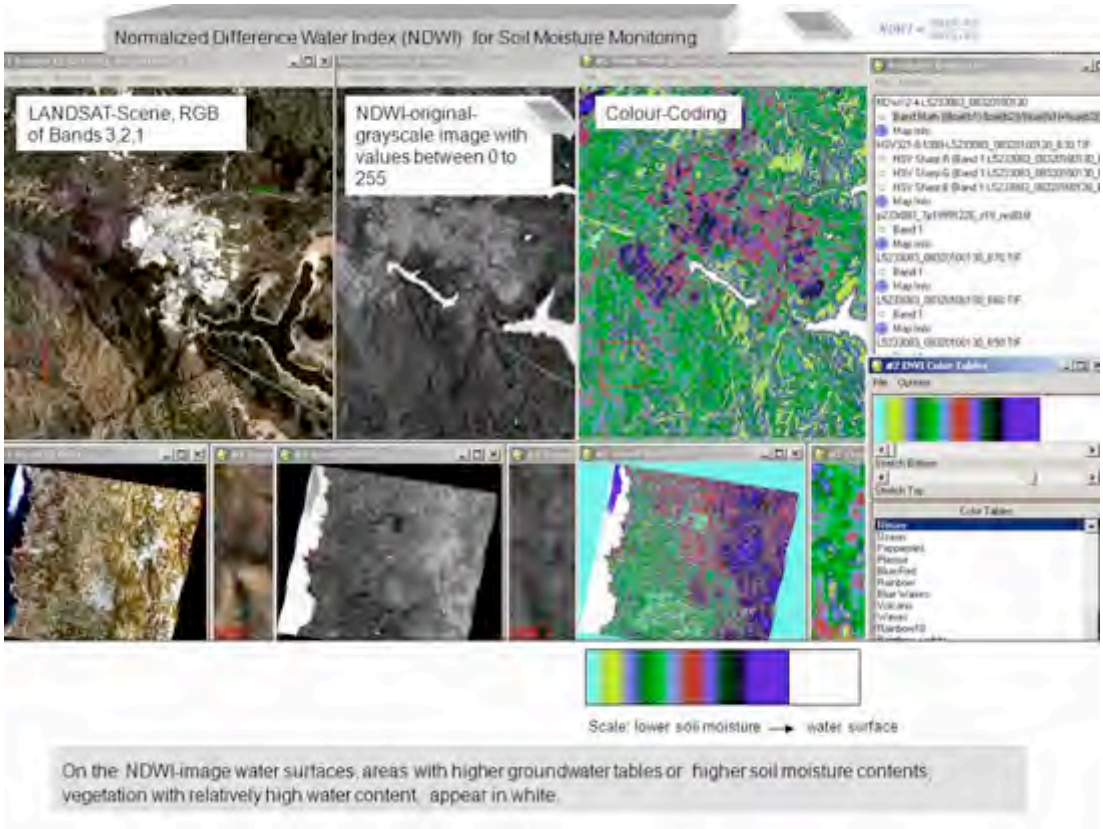

Fig. 5: Water index calculation

After calculating the NDWI in ENVI image processing software an image product with greyscale values between 0 and 255 was created. The NDWI values were ranging from zero to 255 by assigning the least NDWI value in each image cube a value of zero and the maximum NDWI a value of 255. The image products were histogram-stretched and colour-coded and then loaded/integrated into ArcGIS. The result of the histogram stretching was correlated with the visible surface water. In the visible spectrum, reflectance characteristics of surface water can be detected easily. Surface water and water-saturated soils are represented on the chosen colour table in this case in white (Fig. 5). Plants with relatively higher water content appear white as well. Similar spectral response was observed in some cases from larger buildings or shadows in hilly areas. Therefore a careful analysis is necessary.

The patterns in NDWI values for the regions generally represent the temporal variation of surface water size and contour, surface soil moisture (before leaf on) and vegetation water content. The available images were predominantly captured during dryer seasons to minimise cloud cover. This might lead to an underestimation of the true extent of water bodies and to errors. Sensor technical difficulties such as atmospheric haze, poor sensor calibration for some images and, significantly, shadow effects from high topographical areas lead to an overestimation of the water body extent in areas with strong relief. In almost all techniques for mapping water signatures from satellite imagery, shadow areas are a constant noise as the absorption and reflectance of wavelengths in these areas are almost identical spectrally to the absorption and reflectance of wavelengths by large open water features.

As higher values of the NDWI-calculation generally can be correlated with relatively higher water contents at the surface, with higher groundwater tables and surface water, a request was started in ArcMap selecting all values of the NDWI-gray scale image (values:0-255) above 180,…240, and 250), see Fig. 6. These higher values correspond to water surfaces and soils with high water saturation at the acquisition date of the satellite image, what can be confirmed by the visual evaluation of RGB-imageries. This approach, thus, contributes to the detection and the visualization of areas that are more susceptible - in case of a stronger earthquake - to secondary effects such as compaction, liquefaction or soil amplification.

3.2.3. Evaluations of LANDSAT Thermal Bands

An important part of this study was the evaluation of the Thermal Bands 6 of LANDSAT data. All free available, cloud-free LANDSAT data from the USGS and the Global Land Cover Facility of the University of Maryland from 1972 to 2011 were digitally processed. When colour-coding the thermal LANDSAT bands from the coastal area of Valparaiso, water currents at the acquisition time become clearly visible. Of course, these images almost reflect the water, wind and temperature conditions at the data acquisition time. Nevertheless, the streaming pattern visible on the LANDSAT imageries provides some useful information of the influence of coastal morphology on water currents that might be of interest for the better understanding of tsunami wave propagation. These imageries were merged with bathymetric maps of this area in order to investigate whether the sea bottom topography might be traced by the water current pattern at the sea surface (Fig. 7).

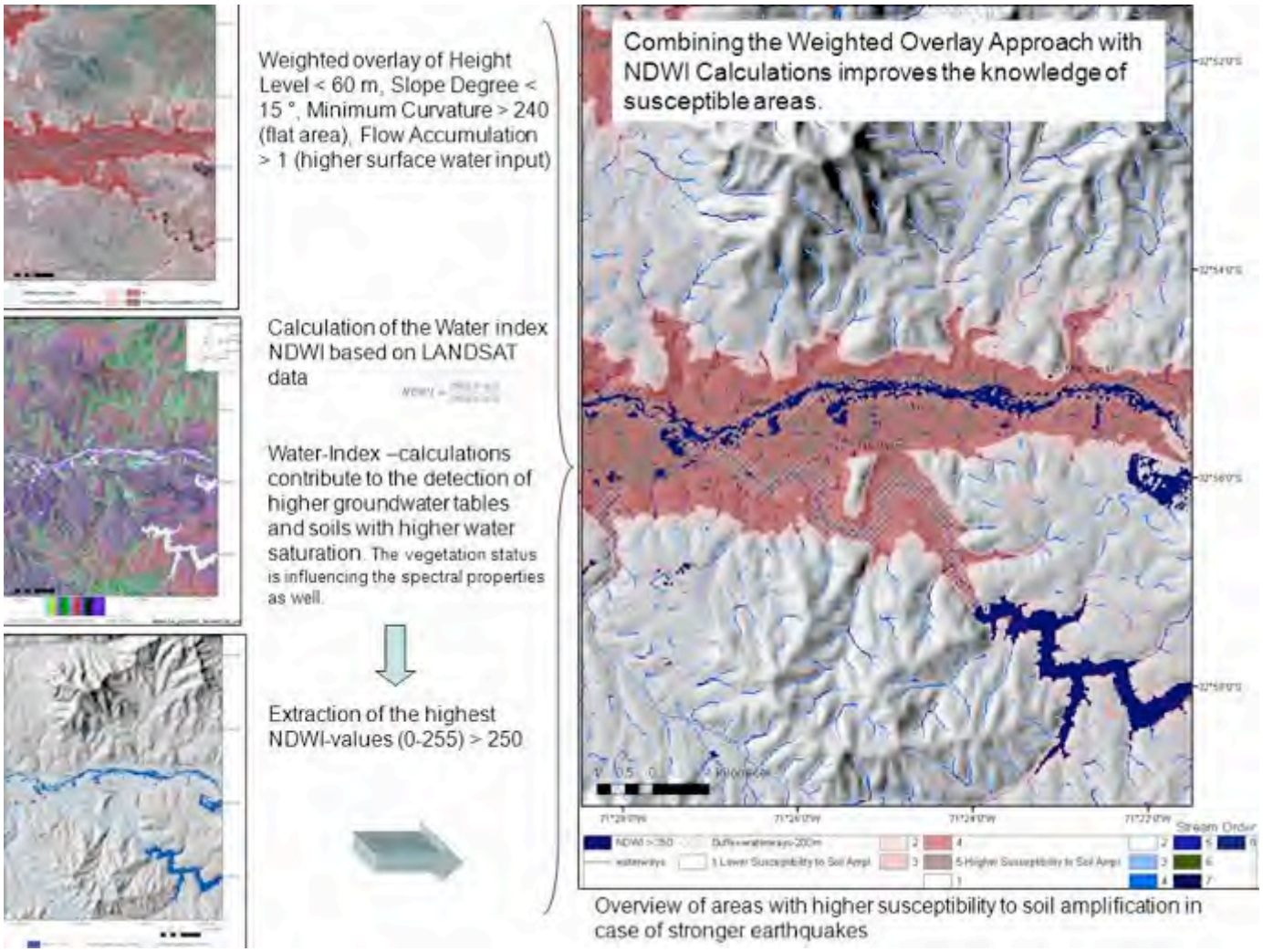

Fig. 6: Normalized Difference Water Index (NDWI) calculation based on LANDSAT TM data and extraction of highest value

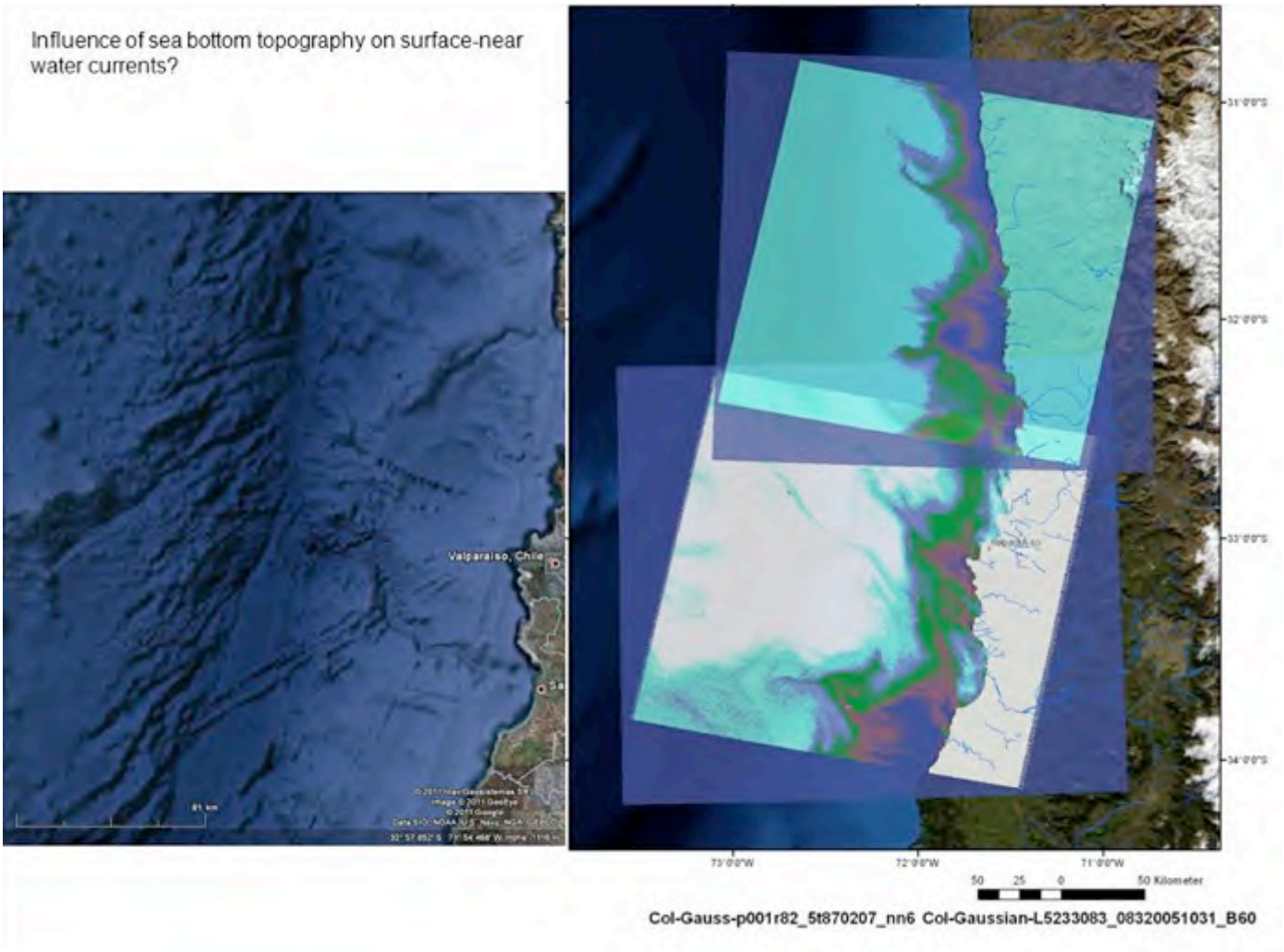

Fig. 7: Colour-coding the Thermal Bands 6 of the LANDSAT satellite data in ENVI software

4. RESULTS OF THE GIS INTEGRATED EVALUATIONS OF REMOTE SENSING DATA

4.1. Results of the Weighted Overlay Methods

After evaluating the ASTER and SRTM DEM data, gaining morphometric maps, extracting causal factors with influence on local site conditions as shown in Fig. 3. Using the weighted overlay tool in ArcGIS, an overview of areas more susceptible to soil amplification in case of stronger earthquakes can be obtained. Comparing these results with geologic maps, it can be stated that these areas correspond to outcrops of unconsolidated, Quaternary sediments. The following figures demonstrate these areas in red to dark-red colours (Figs. 8 and 9).

Lineaments mapped based on the LANDSAT images are included into the maps in order to get more information of the structural pattern and its potential influence on seismic wave propagation, and of active shear zones with movements.

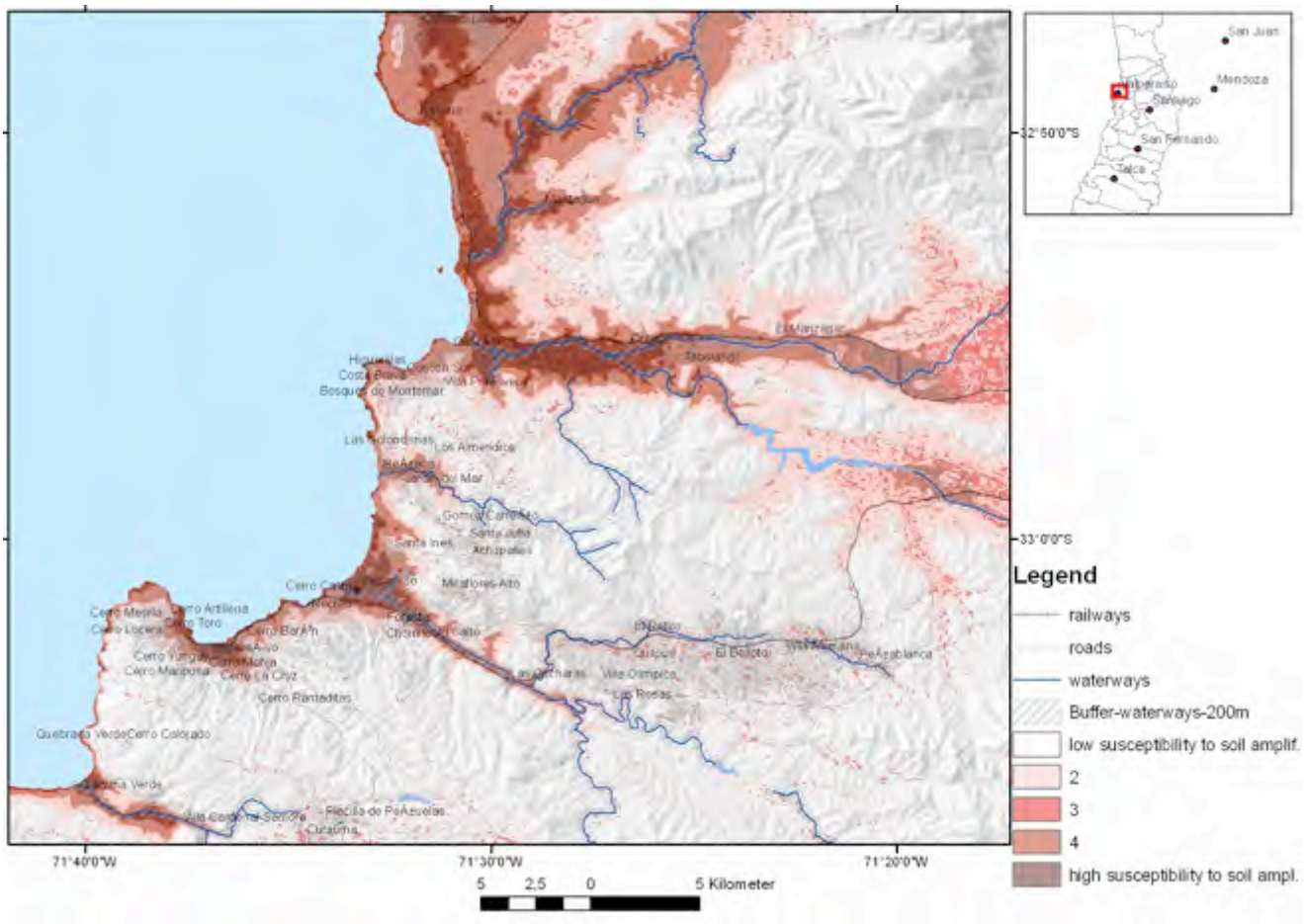

Fig. 8: Susceptibility to soil amplification according to the weighted-overlay-method based on ASTER DEM data

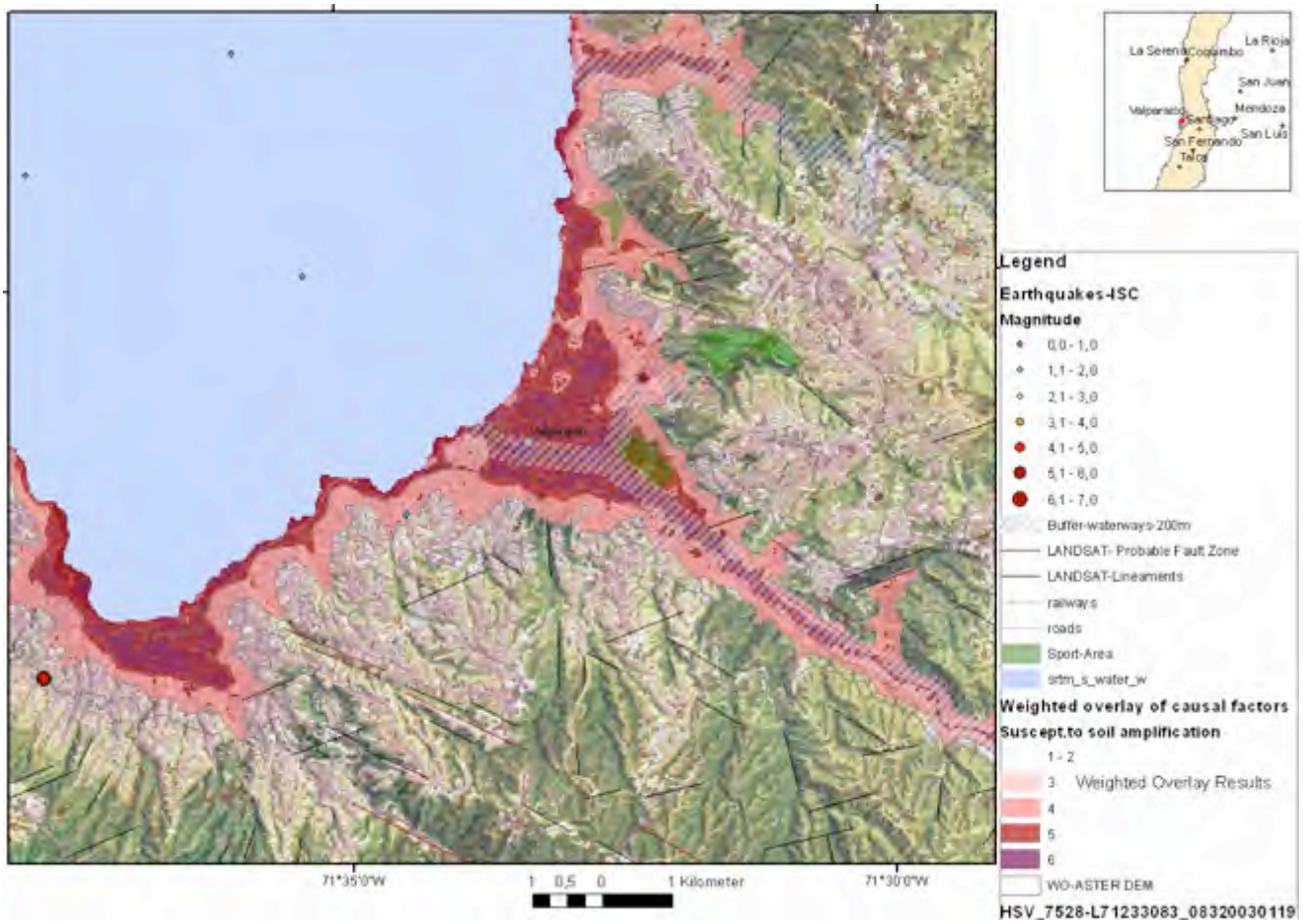

Fig 9: Susceptibility to soil amplification according to the weighted-overlay-method based on ASTER DEM, LANDSAT data, geologic maps and earthquake data

Aggregating following factors: [height level < 10m] + [slope degree < 10°] + [curvature = 0] + [flow accumulation >1] + [outcrop of Quaternary sediments-Grid] + [fault zones-Grid] Dark-red areas correspond to the areas where nearly all "causal" factors overlap.

ShakeMaps showing the distribution of recorded peak ground acceleration (PGA) and peak ground velocity (PGV) overlain on regional topography maps allow to gauge the effects of local site amplification because topography is a simple proxy for rock versus deep-basin soil-site conditions. This can lead to more detailed investigations into the nature of the controlling factors. Peak velocity values are contoured for the maximum horizontal velocity (in cm/sec) at each station. (PGA is peak ground acceleration in units of %g, PGV is peak ground velocity in units of cm/s). Typically, for moderate to large events, the pattern of peak ground velocity reflects the pattern of the earthquake faulting geometry, with largest amplitudes in the near-source region, and in the direction of rupture (directivity). Differences between rock and soil sites become apparent (USGS, access: 2011).

The following figure shows an overlay of shake maps from larger earthquakes with the weighted overlay results (Fig.10). The combination of these two approaches allows a better overview of areas probably prone to higher earthquake shock due to local site conditions within one calculated shake zone.

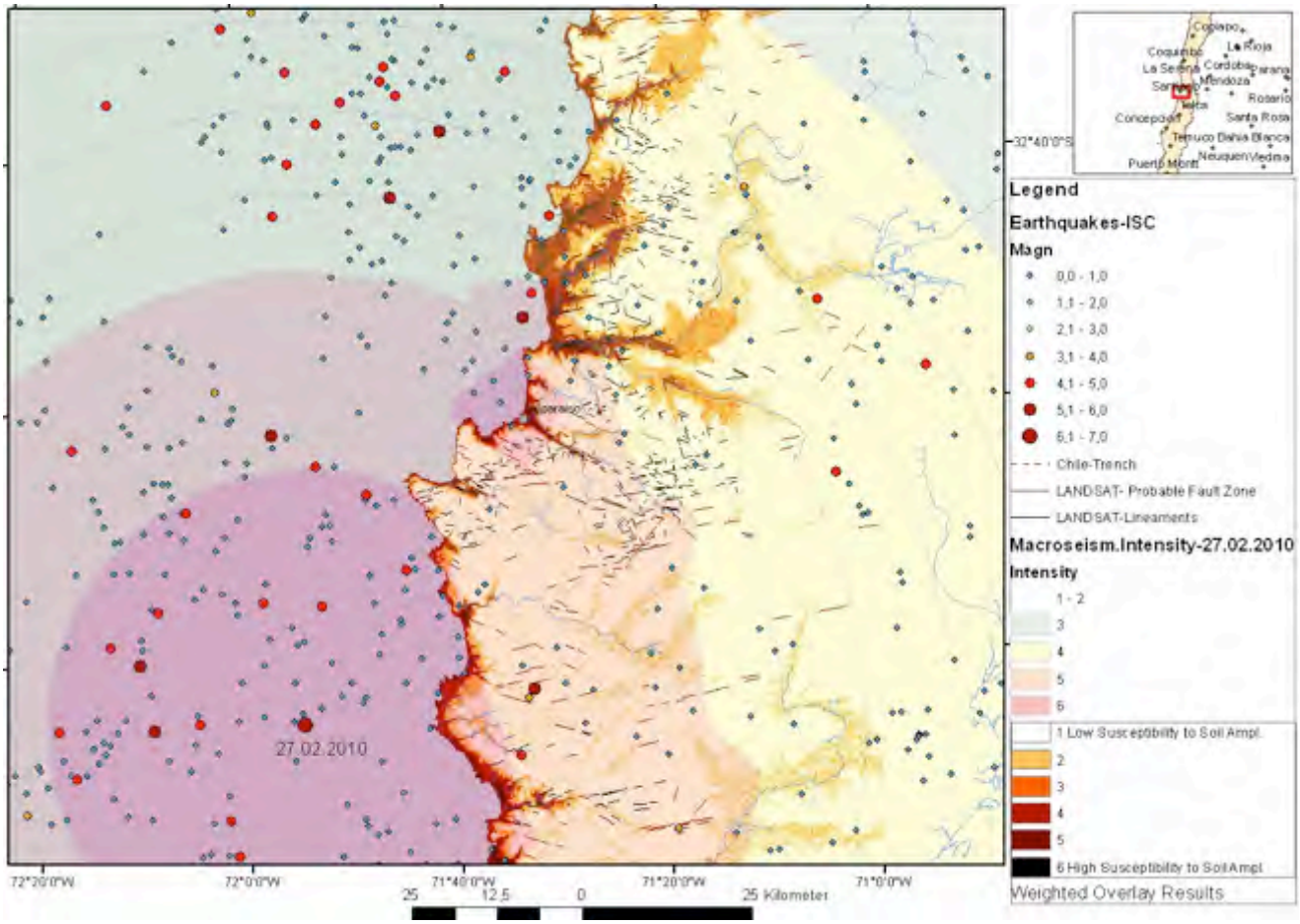

.

Fig. 10: Overlay of the macroseismic intensity-map (shakemap according to USGS) with the results of the weighted overlay calculations of morphometric factors influencing local site conditions based on ASTER DEM data

4.2. Evaluation Results based on LANDSAT image data

The structural evaluation of the LANDSAT images allows the detection of linear features due to their morphologic expression and/or linear tone anomalies. Using the filter tools in ENVI the detection of the lineaments was improved. Fig. 11 shows the results of the water index calculations based on LANDSAT data of different years and seasons. The varying water content in the plants and soils becomes clearly visible.

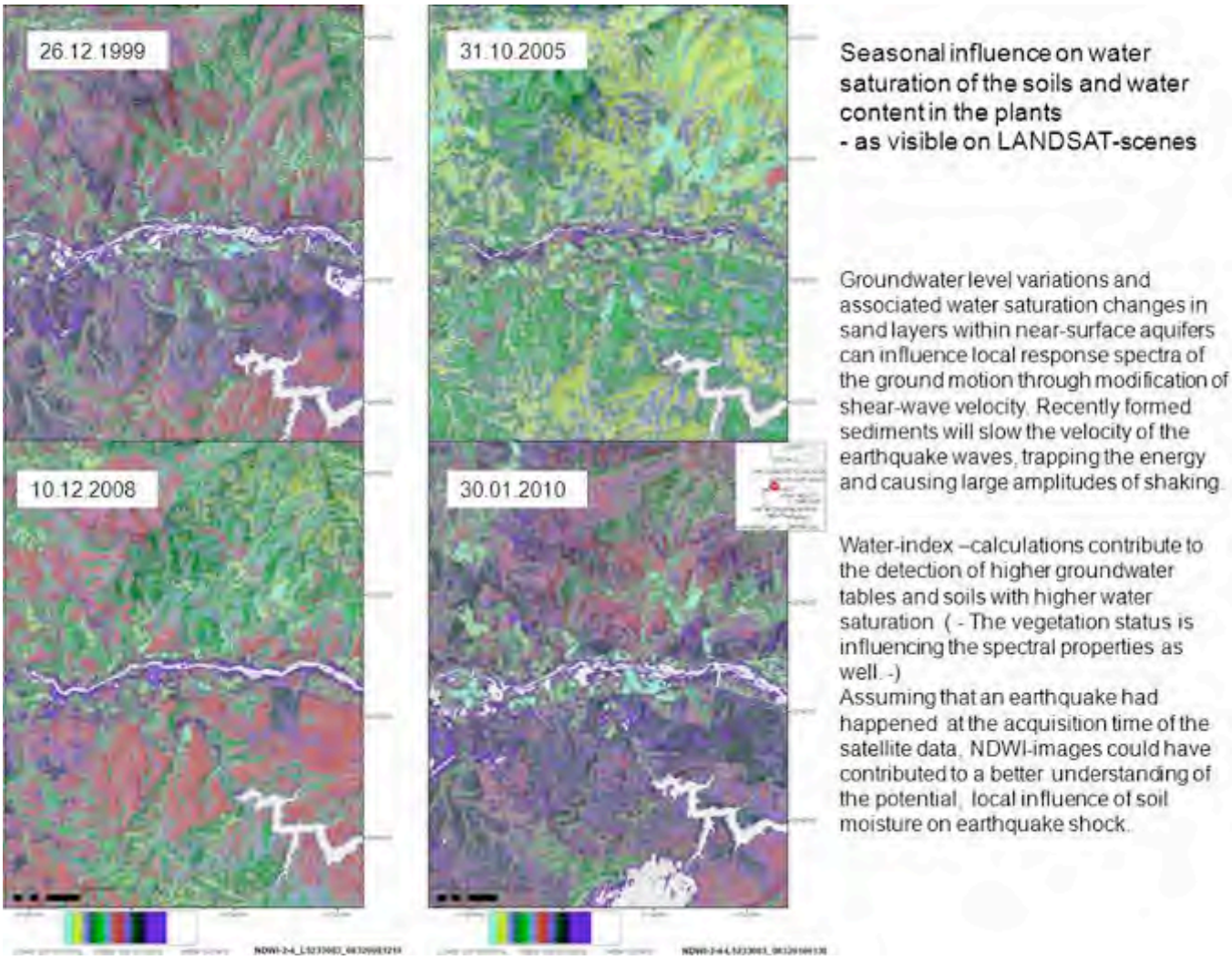

Fig. 11: NDWI calculations based on LANDSAT imageries of different seasons and years for visualizing seasonal variations.

The highest NDWI values were extracted and merged with the weighted overlay results (Fig. 12). Whenever a stronger earthquake occurs, NDWI calculations based on at the same time available image data like RapidEye or Sentinel data can quickly provide an overview of the soil moisture conditions that might have an influence on earthquake shock intensity.

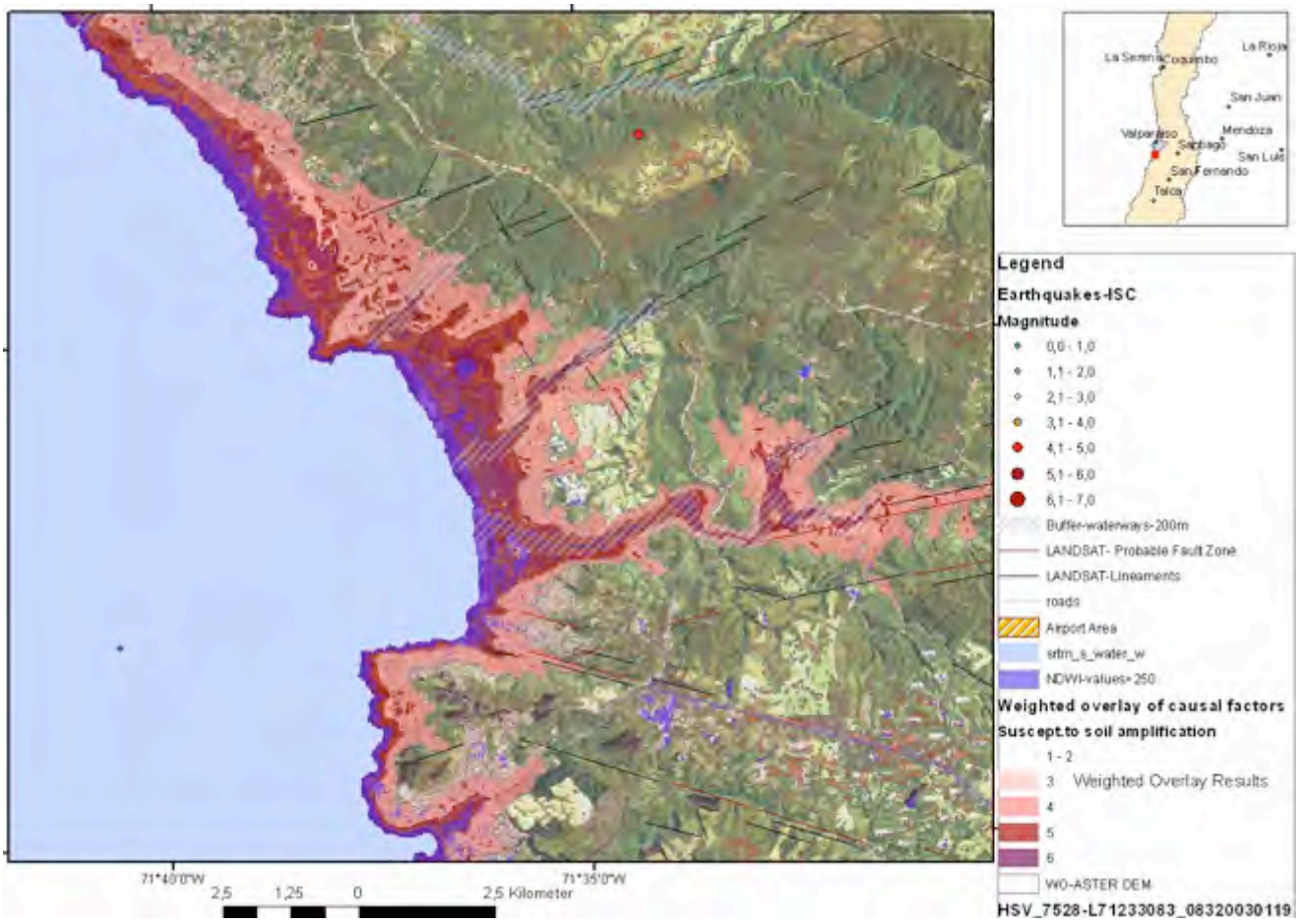

Fig.12: Extraction of the highest NDWI-values (lila) based on different LANDSAT data for visualizing potential influences of soil moisture on earthquake shock intensity

5. SHEAR WAVE VELOCITIES

Shear-wave velocity is an important factor when investigating local soil conditions. A standardized approach for mapping seismic site conditions measuring or mapping shear-wave velocity (*V*S) was developed by Wald & Allen (2007). As in many seismically active regions of the world, information about surficial geology and *V*S either, does not exist, varies dramatically in quality, varies spatially, or is not easily accessible Wald & Allen first correlated *V*S 30 (here V_S^{30} refers to the average shear-velocity down to 30 m) with topographic slope (m/m) at each *V*S 30 measurement point for data. The basic premise of the method is that the topographic slope can be used as a reliable proxy for V_{S30} in the absence of geological and geotechnical based site-condition maps through correlations between V_{S30} measurements and topographic gradient. By taking the gradient of the topography and choosing ranges of slope that maximize the correlation with shallow shear-velocity observations, it is possible to

recover, to first order, many of the spatially varying features of site-condition maps. It is worth noting that the resolution (30 arc sec) of the topography allows relatively detailed maps of site conditions. Many of these details come from small-scale topographic features that are likely to be manifestations of real site differences, such as basin edges and hills protruding into basins and valleys - and are thus easily visible due to their significant slope change signatures. Typically, these edges are important for predicting ground motion variations due to earthquakes (Wald and Allen, 2007). Thus, from the Valparaiso area the derived Vs (m/sec) data were downloaded from the USGS and integrated and interpolated in ArcGIS for getting an overview of the estimated shear velocities in case of larger earthquakes (Fig. 13). Lower shear wave velocities up to 400 m/s as derived by Wald & Allen correspond quite well with the outcrop of unconsolidated, Quaternary sediments in the broader valleys. Merging the Weighted-Overlay-Susceptibility map with the Vs-data derived by Wald and Allen (2007) there is a coincidence of areas assumed to be more susceptible to soil amplification according to the weighted overlay approach with areas of estimated lower shear wave velocities (Vs < 250, Fig.14).

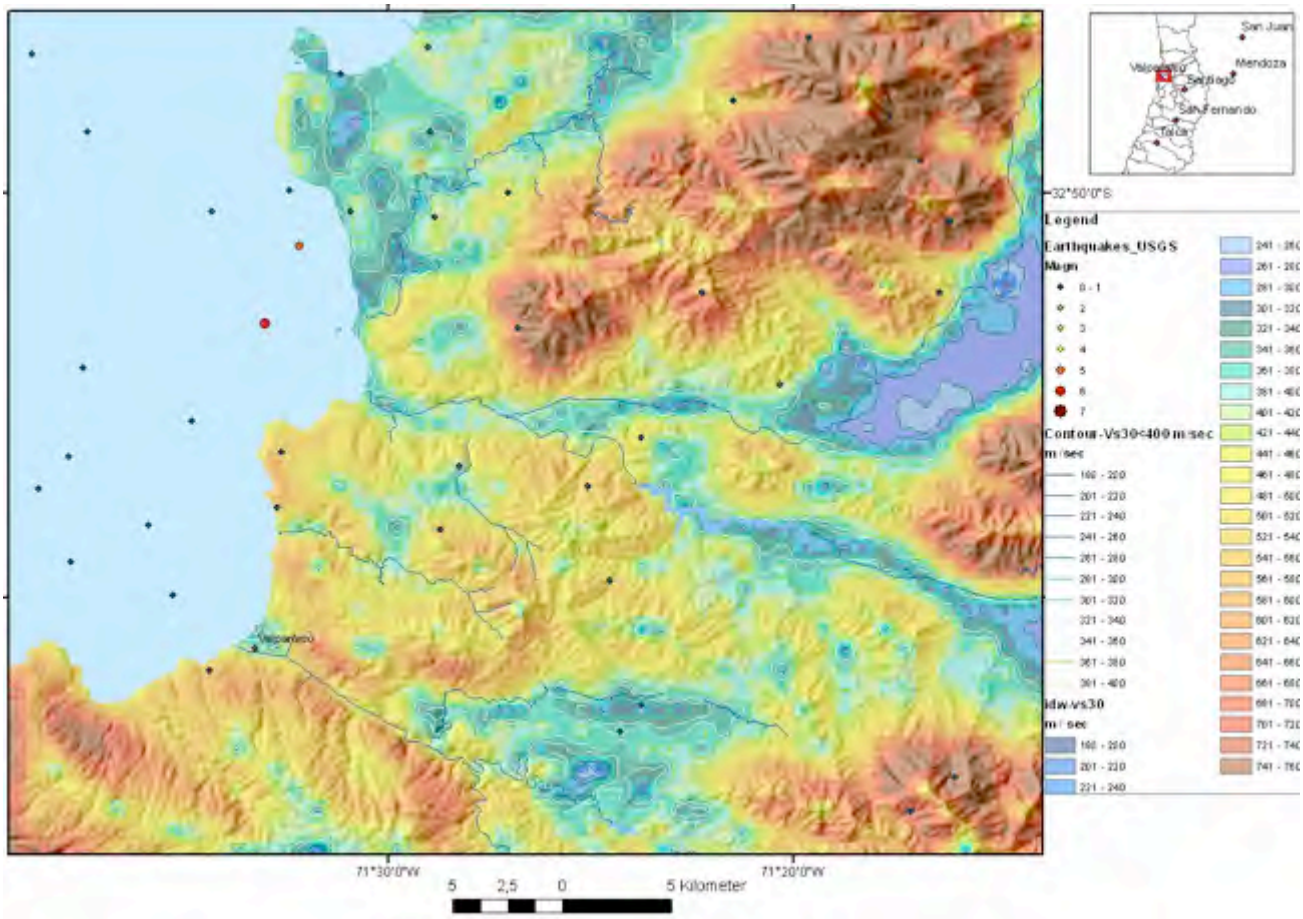

Fig. 13: Estimated shear wave velocities (Vs) in the Valparaiso-area area as derived by Wald and Allen (2007)

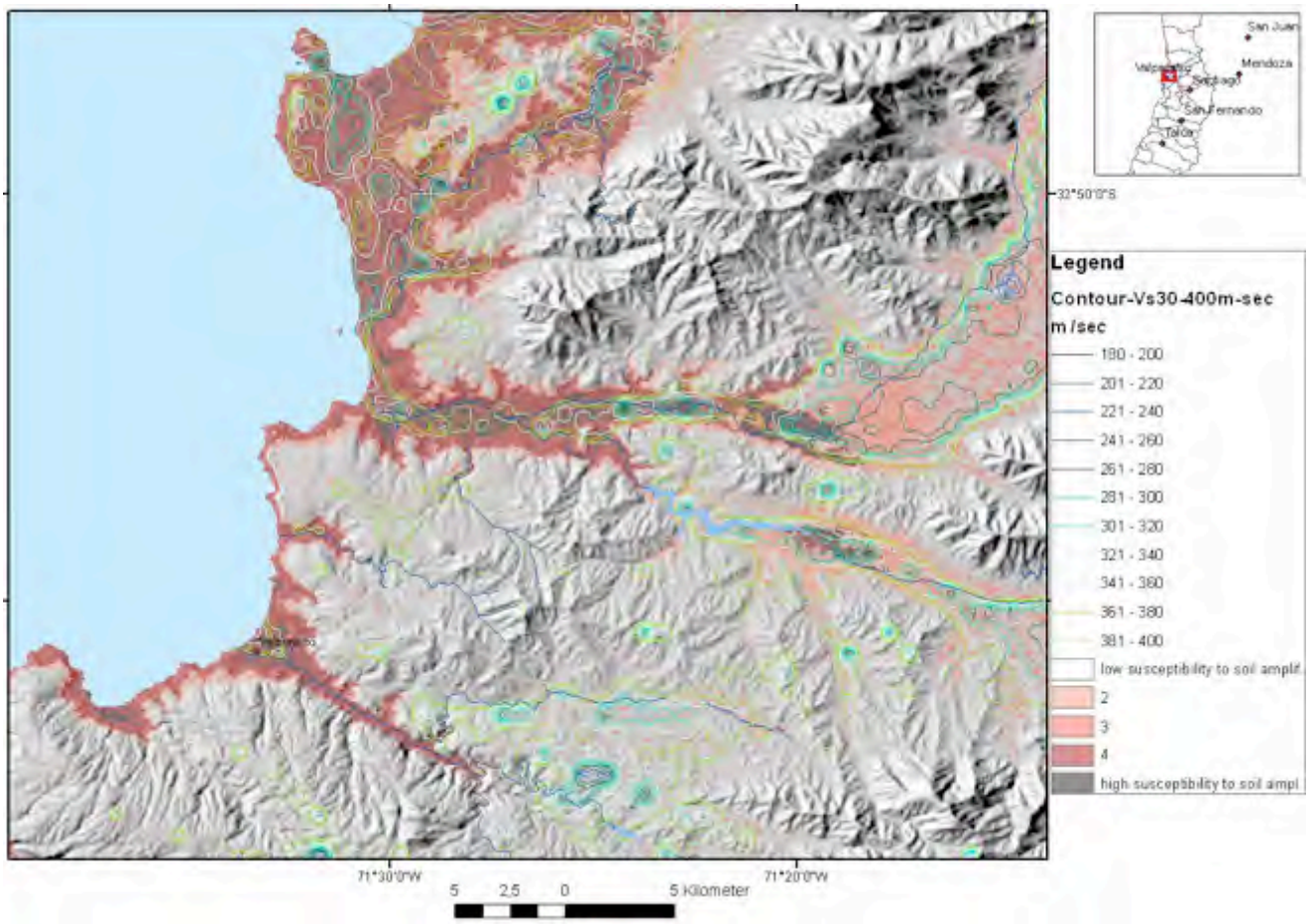

Fig.14: Merging assumed shear velocity data (Vs30 < 400 m/sec) from USGS as contour lines with the soil amplification susceptibility map according to the weighted overlay-approach.

6. FLOODING SUSCEPTIBILITY

The Chilean coast is currently exposed to the effects of near and far field tsunamis generated in the Pacific Ocean (Gutierrez, 2005). Tsunami waves have been documented after various larger earthquakes (Figs. 1 and 15). For instance, the catastrophic events of the last century, in 1868 and 1877, overwhelmed the coast of the northern region of the country. In the younger history there are 6 earthquakes related with the occurrence of tsunami waves in the Bay of Valparaiso: 13.05.1647, 08.07.1730, 19.11.1822, 16.08.1906, 03.03.1985 and 27.02.2010 (Pararas-Carayannis, 2010). During this century, the most important disaster was the 1960 earthquake and tsunami in Valdivia. An overview of tsunami events in Chile is provided by NOAA's Satellite and Information Service (NESDIS) and by the Servicio Hidrografico y Oceanografico de la Armada de Chile.

The planning of economic activity and any new constructions in these seismically active and tsunami risk zones of the Chilean coast requires preliminary estimates of the possible flooding extent related to tsunamis. Most tsunamis are generated by submarine earthquakes, also by inland /coastal earthquakes, turbidity currents and landslides. Tsunami propagation is sensitive to sea bathymetry. Tsunami impact on the coast and flooding is influenced by coastal topography. Ridges rising from the ocean floor such as seamounts/guyots, or deeper canyons, may have an influence of the tsunami energy propagation. In case of storm floods or stronger tsunami events the coastal morphology and islands will modify the flooding dynamics. The interaction of tsunami waves with local elements is governed by the geometrical scale of the obstacles.

Based on the aforementioned geospatial data sets, a number of tsunami hazard-controlling parameters are derived, including elevation, slope, aspect, curvature, concavity, soil types, land use classification, and hydrological variables (drainage density, flow accumulation and flow path). By using GIS-based map overlay techniques, the derived tsunami susceptibility values are the weighted linear summation of the controlling or causal factors such as slope, curvature, flow accumulation, soil type, soil texture, elevation, vegetation cover and drainage pattern.

Summarizing factors influencing flooding susceptibility such as relatively lowest height levels (< 10 m), minimum terrain curvature (values=0), slope gradients below 10° and high flow accumulation values using the weighted-overlay tools in ArcGIS helps to map areas susceptible to flooding, see Fig. 15. As river mouths form an entrance for flooding waves, those areas along the river sides are even more susceptible to flooding, visualized in the GIS by a 100 m and 200 m-buffer-layer along the waterways.

The evaluation of LANDSAT imageries can contribute to a better understanding of surface-near water streaming mechanisms. When colour coding and classifying LANDSAT imageries of different acquisition dates water currents become visible (Figs. 16 to 18). The colour-coded thermal imageries provide an overview of the different streaming pattern during the image acquisition. Merging the thermal imageries with the bathymetric map, it seems that subsurface structures as canyons and terraces influence even the near-surface water streaming (Figs. 19 and 20). Especially above submarine canyons, water currents can be observed. In case of tsunami waves it can be assumed that the coastal morphology could cause similar effects.

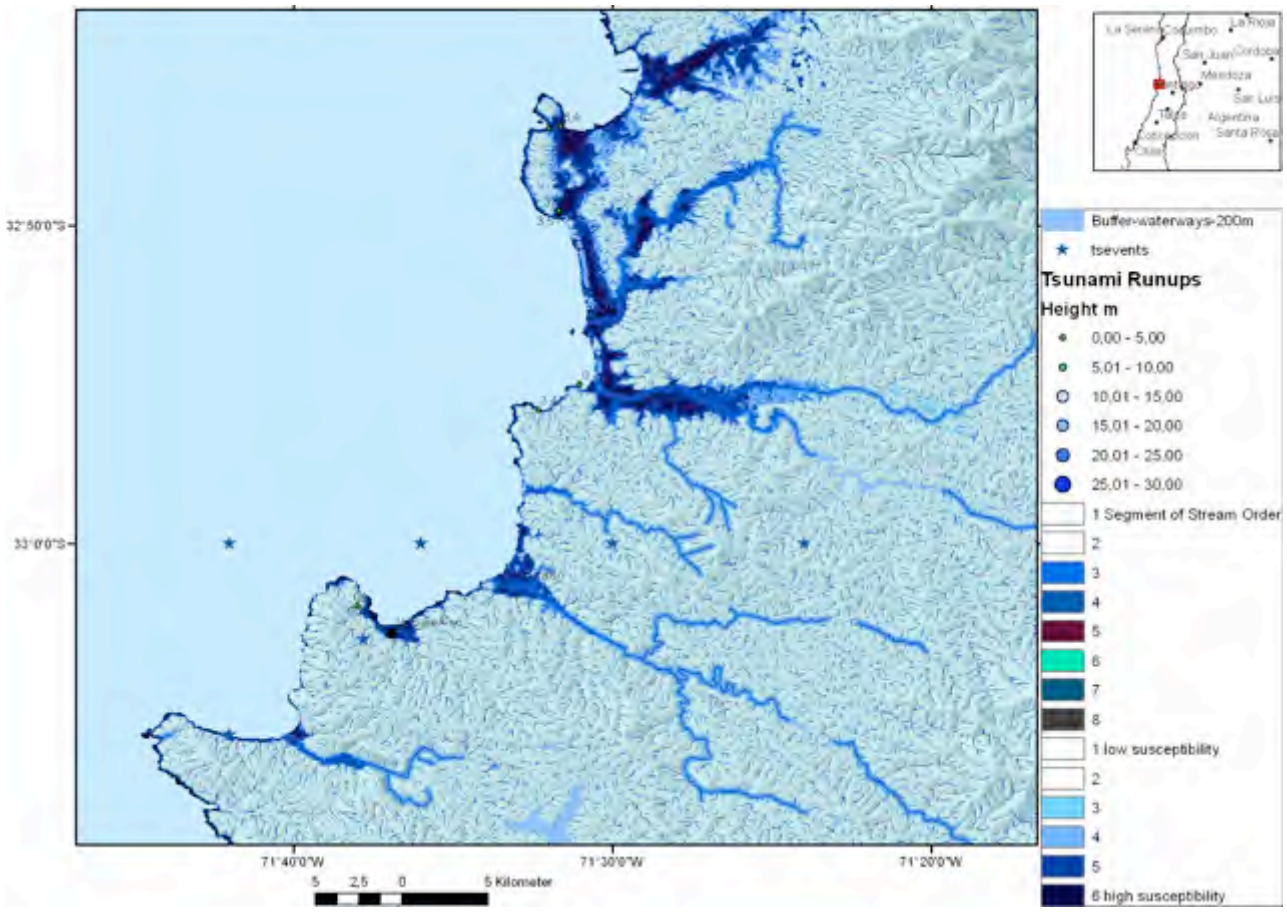

Fig. 15: Flooding susceptibility map of Valparaiso in case of storm surges, flash floods or tsunami waves based on the aggregation of the following factors (based on SRTM DEM) using the weighted overlay-tool of ArcGIS: [height level <5- 10 m] + [slope degree < 10°]+[curvature=0]+ [high flow accumulation]+ river mouths and estuaries-Grids, Buffer of 200 m along the waterways.

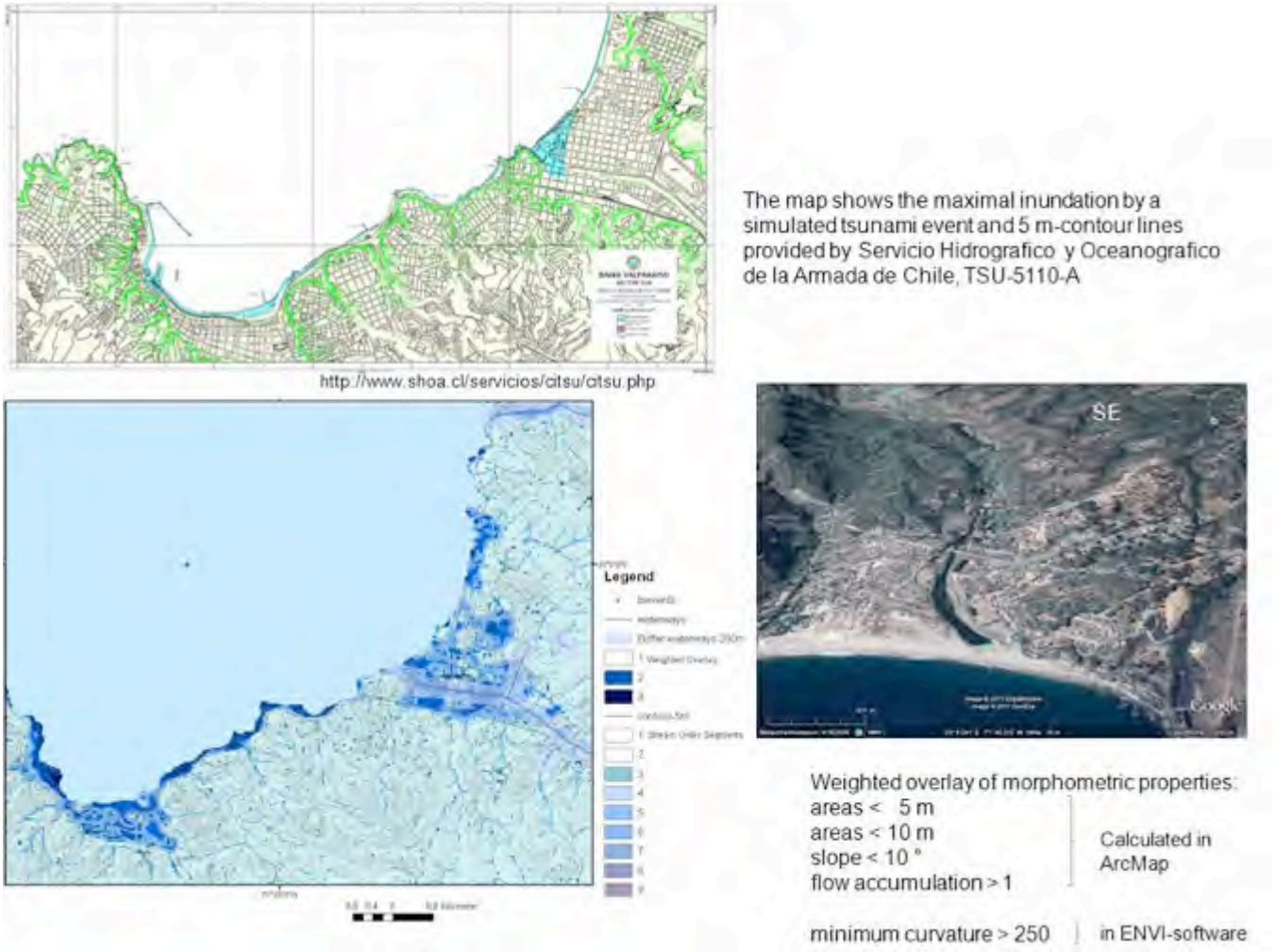

Fig. 16. Comparison of the weighted overlay results (based on ASTER DEM data) and a simulated tsunami inundation map of Valparaiso

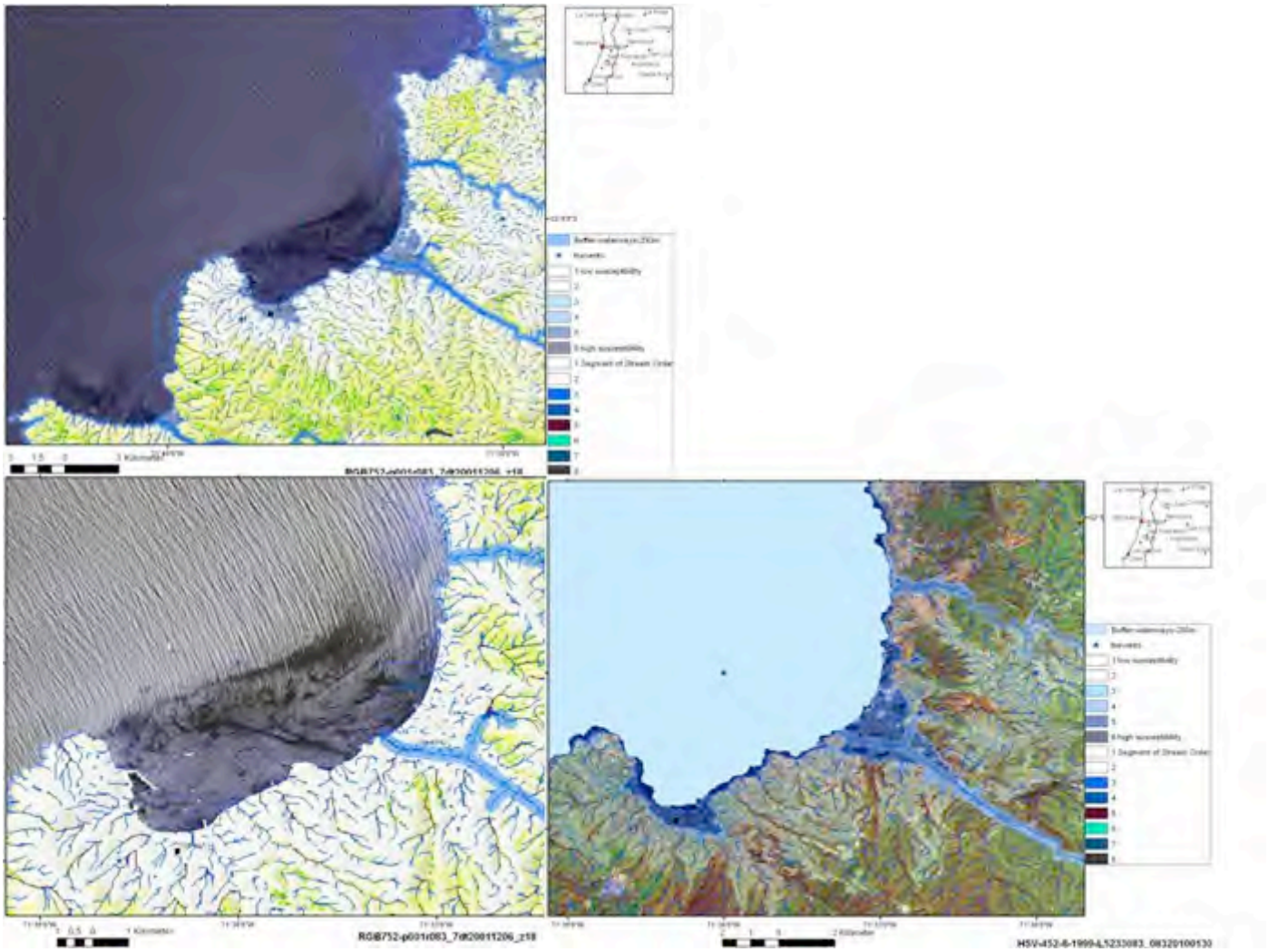

Fig. 17: Wind driven surface waves at the coast of Valparaiso and areas susceptible to tsunami flooding

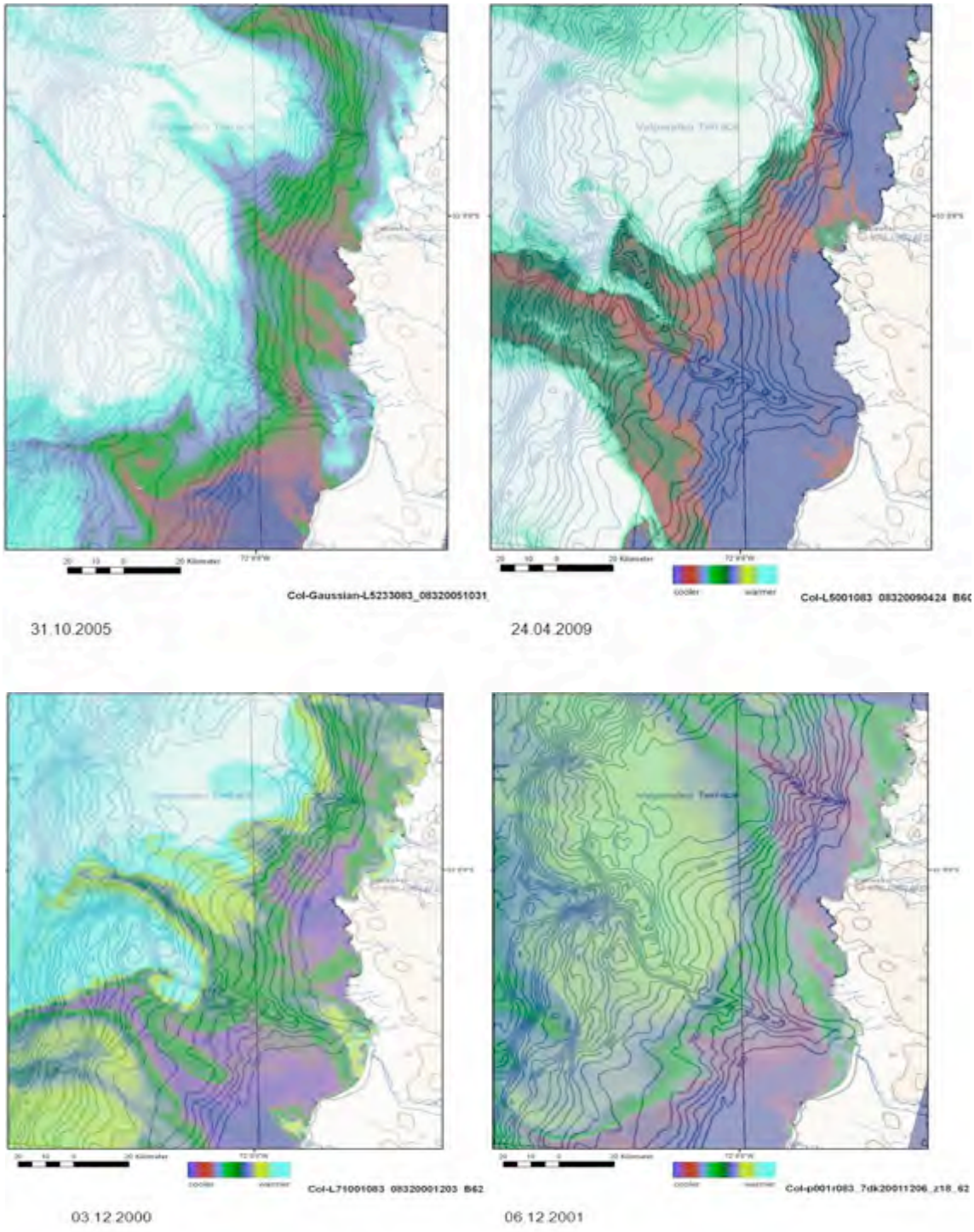

Fig. 18 a, b: Influence of subsurface-topography on surface-near water currents. Comparison of the bathymetric map and colour-coded LANDSAT Band 6-imageries

The concentration of larger fault zones and fault and fracture zones intersecting each other are important factors influencing slope instability onshore and offshore. The almost detailed detection of those larger offshore faults, especially when active, based on geophysical, geodetic and bathymetric data is most important, as these areas might be potential tsunami source regions.

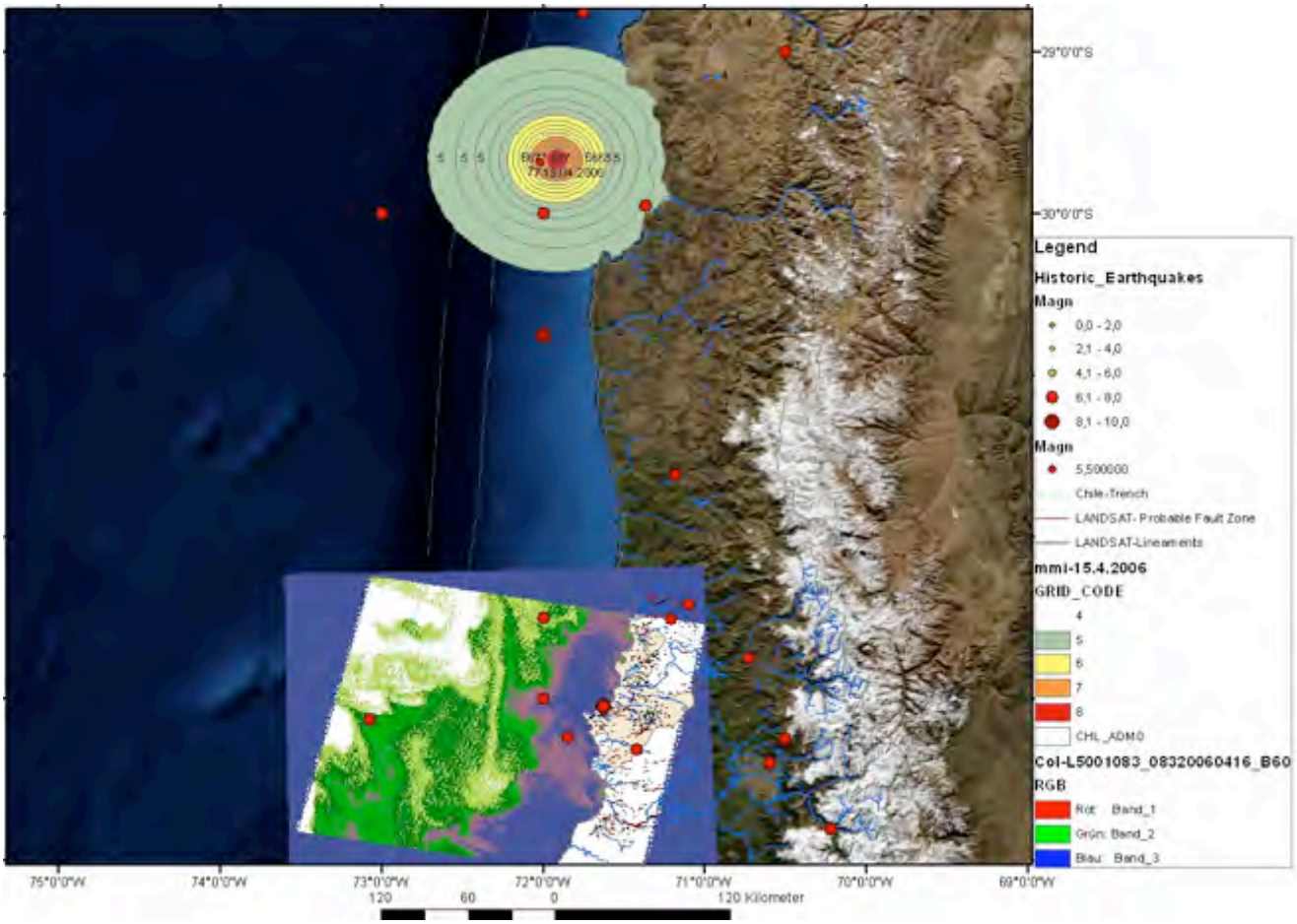

Fig. 19: Earthquake / tsunami (?) induced changes in the surface-near streaming pattern. According to USGS a stronger earthquake (M 6) happened a day before this image was taken.

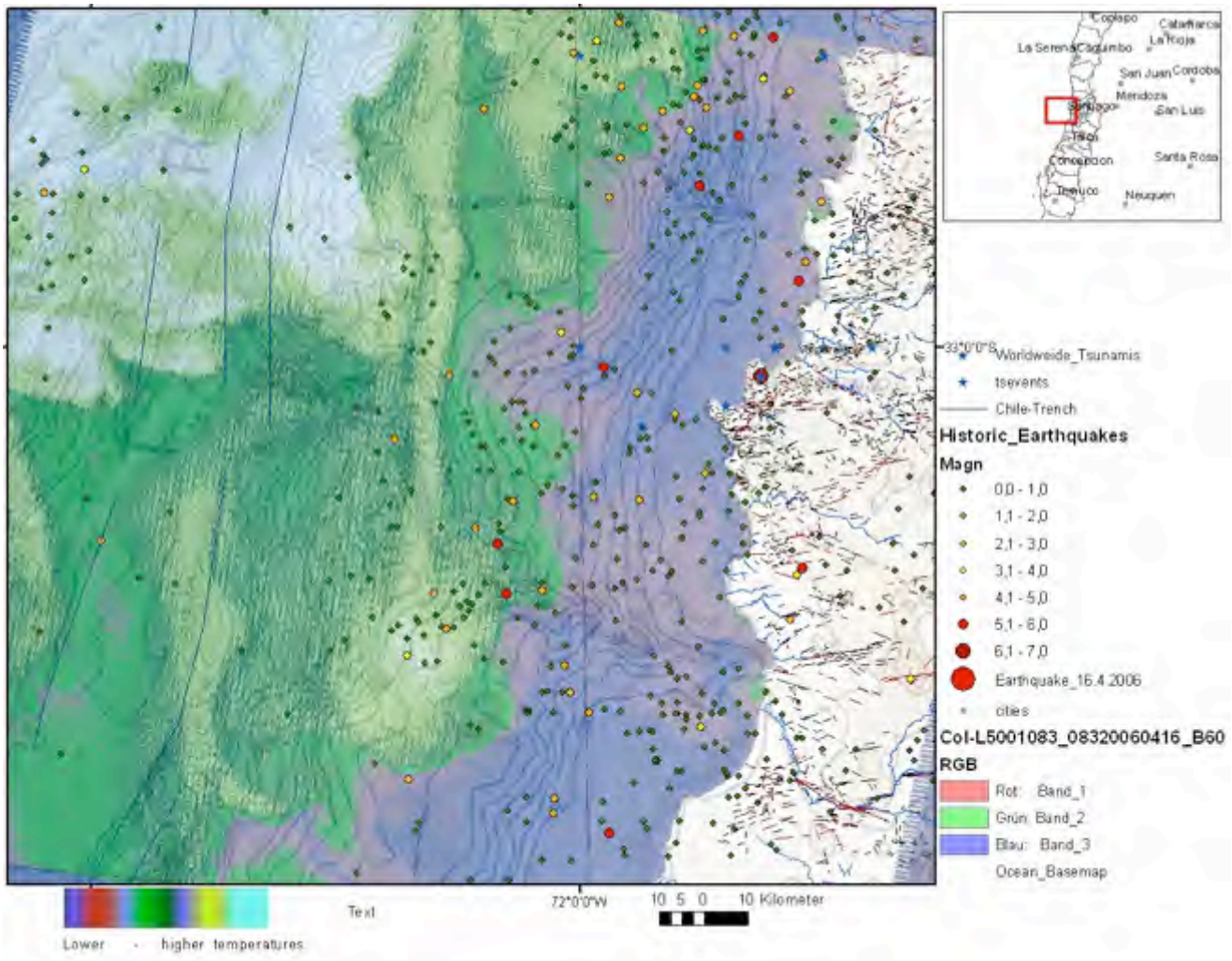

Fig. 20: Sea-surface temperature anomalies on 16.04.2006

7. SUSCEPTIBILITY TO SLOPE FAILURE

After larger earthquakes newly formed landslides were observed (USGS, 1985). The mountainous areas were subjected to landslides after the quake shattered exposed areas, especially those that were prone to previous slope failure in the past. Areas susceptible to slope failure that could be affected by stronger earthquakes should be considered when planning the rebuilt of affected cities. Identification and mapping of instability factors having a relationship with the slope failures require knowledge of the main causes of landslides. These instability factors include lithologic properties of the surface rocks and soil properties, the tectonic pattern, seismicity, slope steepness and curvature, stream evolution, groundwater conditions, climate conditions, vegetation cover and land use.

Figure 21 shows the result of the Weighted-Overlay-aggregation of these main preparatory factors and lineament analysis. Causal or preparatory factors such as steep slopes, convex curvatures, height levels, drainage pattern and lineaments were extracted from recent LANDSAT ETM-, Google Earth- and ASTER- satellite data.

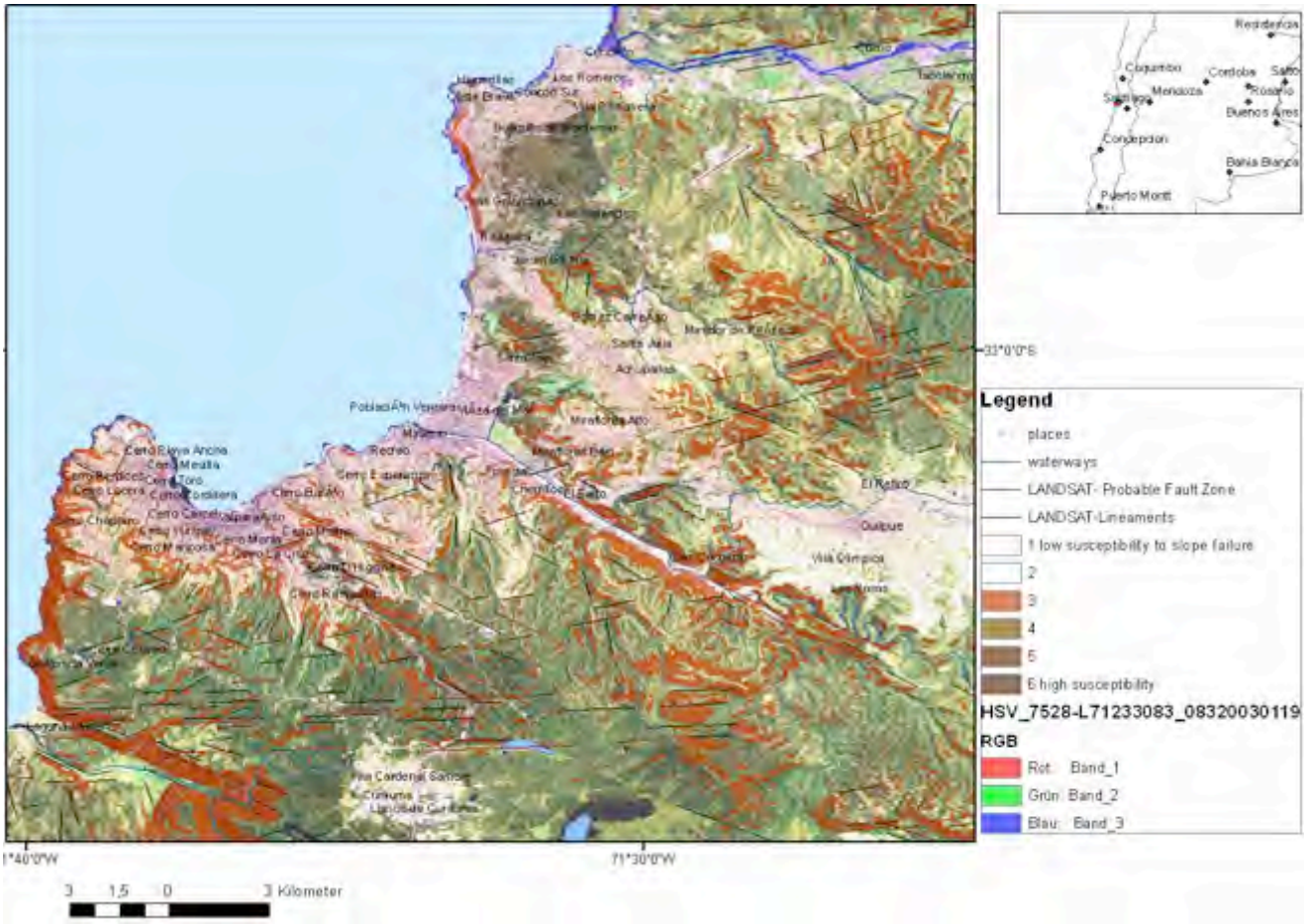

Figure 21: Weighted overlay calculation of some of the causal factors influencing slope stability based on ASTER DEM and LANDSAT data (weighted overlay of: [slope degree >40°] + [maximum curvature > 150]+ [height level > 500 m] + [fault zones-Grid]) and merging the weighted overlay results with LANDSAT data

The susceptibility to slope failure is assumed to be higher in areas of intersecting lineaments.
This approach of landslide susceptibility mapping is valid for a generalized assessment purpose. However, it is less useful on the site-specific scale, where local geological and geomorphologic heterogeneities prevail. Nevertheless this approach contributes to a better overview and understanding of the relationships between the different causal factors and helps to prepare more detailed investigations in the field.

8. CONCLUSIONS

The nearly world-wide available SRTM and ASTER-DEM data and LANDSAT imageries support a standardized, low-cost to no cost approach for the detection of some of the near-surface, causal factors of local site conditions influencing earthquake shock and damage intensity, as well as of factors influencing earthquake related secondary effects. A standardized procedure for mapping and assessing earthquake damage susceptibility has been developed based on the weighted overlay-approach, which can serve to improve the efficiency of disaster monitoring, management and preparedness. This approach integrates many types of data and geo-processing tools that can automate the processes in an efficient manner. Aggregating factors influencing the surface-near earthquake ground motion in a GIS environment allows a first overview of areas with probably higher susceptibility to soil amplification, slope failure and flooding. The advantage of GIS is that the system is open and additional data can be integrated as layers as soon as additional data are available. Thus, remote sensing data and GIS integrated evaluations and analysis can contribute to a better planning of cost and time-intensive geotechnical measurements that are important to consider. The derived results from the whole process provide essential information for immediate response when future disasters will occur.

Acknowledgements

The support of EU, FP 7, Large Collaborative Research Project, IRIS - Integrated European Industrial Risk Reduction System, CP-IP 213968-2, is kindly acknowledged.

REFERENCES

Allen, T. & Wald, D.: On the Use of High-Resolution Topographic Data as Proxy for Seismic Site Conditions (V_{S30}), Bulletin of the Seismological Society of America*;* April 2009; v. 99; no. 2A; p. 935-943,2009. DOI: 10.1785/0120080255

Calais, E., Mazabraud, Y., de Le´pinay, M.B., Mann, P., Mattioli, G. and Jansma, P.: Strain partitioning and fault slip rates in the northeastern Caribbean from GPS measurements, Geophysical Research Letters, VOL. 29, No. 18, 1856, doi:10.1029/2002GL015397, 2002.

Dolan, J., and Wald, D.: The 1943–1953 northcentral Caribbean earthquakes: Active tectonic setting, seismic hazards, and implications for Caribbean-North America plate motions, in Active Strike-slip and Collisional Tectonics of the Northern Caribbean Plate Boundary Zone*,* edited by J. Dolan and P.Mann, Geol. Soc.Am.Spec.Pap. 326, pp.143–169, Geological Society of America, Boulder, 1998.

Ehret, D.& Hannich, D.: Seismic Microzonation based on Geotechnical Parameters – Estimation of Site Effects in Bucharest (Romania). EOS Trans. AGU, 85 (47), Fall Meet. Suppl., Abstract S43A-0972; San Francisco, 2004.

Ehret, D. ; Kienzle, A. ; Hannich, D. ; Wirth, W. ; Rohn, J. ; Czurda, C.: Seismic microzonation based on geotechnical parameters - estimation of site effects in Bucharest (Romania). In: *Geophysical Research Abstracts; European Geosciences Union* 6 (2004), Nr. 6, S. 3708-3709

Hannich, D., Hötzl, H. & Cudmani, R.: Einfluss des Grundwassers auf die Schadenswirkung von Erdbeben – ein Überblick. Grundwasser,Vol.11,4, 286- 294,2006.

Giardini, D.,Wiemer S., Fäh D. & Deichmann, N.: Seismic Hazard Assessment of Switzerland,2004.- Swiss Seismological Service, ETH Zürich, Zürich, Switzerland,2004.

Gupta, R.P.: Remote Sensing in Geology, Springer-Verlag, Berlin- Heidelberg-New York, 2003.

Madariaga, R., Métois, M., Vigny, C. & Campos, J. (2010): Central Chile Finally Breaks.- SCIENCE, Vol. 328, 9, APRIL 2010, 181-182

Pararas-Carayannis, G. (2010): The Earthquake and Tsunami of 27 FEBRUARY 2010 in Chile –Evaluation of Source Mechanism and of Near and Far-field Tsunami Effects.- Science of Tsunami Hazards, Vol. 29, No. 2, 96-126

Schneider, G.: Erdbeben- Eine Einführung für Geowissenschaftler und Bauingenieure, Spektrum Akademischer Verlag, München,2004.

SHOA Report "CARTA DE INUNDACION POR TSUNAMI PARA LA BAHIA DE VALPARAISO, CHILE". http://www.shoa.cl/servicios/citsu/citsu.php

Sobiesiak, M. (2004): Fault Plane Structure of the 1995 Antofagasta Earthquake (Chile) Derived From Local Seismological Parameters.- Dissertation, University of Potsdam

Steinwachs M.(1988). Das Erdbeben am 19.September 1985 in Mexiko –Ingenieurseismologische Aspekte eines multiplen Subduktionsbebens, in: Steinwachs M. (ed).: Ausbreitungen von Erschütterungen im Boden und Bauwerk. 3.Jt. DGEB, TransTech.Publications, Claustha1,1988.

Theilen-Willige, B. and Wenzel, H.: Local Site Conditions influencing Earthquake Shaking Intensities and Earthquake related Secondary Effects - A Standardized Approach for the Detection of Potentially Affected Areas using Remote Sensing and GIS-Methods.- 10.Forum Katastrophenvorsorge, Katastrophen – Datenhintergrund und Informationen UN Campus, Bonn, 23. - 24. November 2009. http://188.111.81.194/download/forum/10/Theilen-Willige_Wenzel_ExtAbst.pdf

Theilen-Willige, B., Mulyasari Sule, F.& Wenzel H.: Environmental Factors derived from Satellite Data of Java, Indonesia, in: Christian Boller, Fu-Kuo Chang & Jozo Fujino (Editors): Encyclopedia of Structural Health Monitoring.- John Wiley and Sons,Ltd., Chichester,UK, 2343-2354, 2008.
http://www.jsg.utexas.edu/news/pdfs/011310/Tuttle_et_al_2003_DR.pdf

Wald, D.J. & Allen, T.I.: Topographic Slope as a Proxy for Seismic Site Conditions and Amplification.- Bulletin of the Seismological Society of America, October 2007; v. 97; no. 5; p. 1379-1395,2007. DOI: 10.1785/0120060267

Winckler Grez,P. & Vásquez Álvarez, J. (2008): Evaluacion de Riesgo de Tsunami en Quintero, Chile.-Anales del Instituto de Ingeniería de Chile. DOC ICO 01-2008**,** Vol 120 No 1, Abril 2008, 1-12 (ISSN 0716-2340), www.ingenieriaoceanica.cl/files/200801_**tsunami**_sochid2.pdf

Vigny, C., Rudloff, A., Ruegg, J.-C., Madariaga, R., Camposc, J., & Alvarezc, M.(2009): Upper plate deformation measured by GPS in the Coquimbo Gap, Chile.- Physics of the Earth and Planetary Interiors, 175 (2009), 86–95

Internet sources:

UNOSAT:
http://www.disasterscharter.org/image/journal/article.jpg?img_id=63885&t=1263988941535
USGS, Seismic Hazard Program, Global V_s^{30} Map Server
http://earthquake.usgs.gov/hazards/apps/vs30/
Southern California Earthquake Center, http://www.scec.org/phase3/overview.html
http://earthquake.usgs.gov/earthquakes/shakemap/background.php#accmaps
Earthquake and Tsunami Data free of Charge:
Centro Regional de Sismología para América del Sur (CERESIS), Catálogo de Intensidades, http://www.ceresis.org/producto/inten_ch.htm,
http://www.ceresis.org/portal/serie_sisra.php
NOAA's Satellite and Information Service (NESDIS)
http://www.ngdc.noaa.gov/hazard/data/publications/Wdcse-39.pdf and
Servicio Hidrografico y Oceanografico de la Armada de Chile,
http://www.shoa.cl/servicios/citsu/citsu.php).
BGR, Hannover:
http://www.bgr.bund.de/cln_145/nn_333452/DE/Themen/Seismologie/Seismologie/Erdbebenauswertung/Erdbebenkataloge/Kataloge__Bulletins/kataloge__bulletins__node.html?__nnn=true
LGRB, Freiburg:
http://www.lgrb.uni-freiburg.de/lgrb/Fachbereiche/erdbebendienst
SED - Swiss Seismological Service
International Seismological Centre, http://www.isc.ac.uk/search/custom/index.html
Stress Data of the WSM, http://dc-app3-14.gfz-potsdam.de/pub/stress_data/stress_data_frame.html

http://map.ngdc.noaa.gov/website/seg/hazards/viewer.htm
GFZ Potsdam GEOFON
http://geofon.gfz-potsdam.de/geofon/

Satellite Data free of Charge:

Global Land Cover Facility, University of Maryland:
http://glcfapp.glcf.umd.edu:8080/esdi/index.jsp
NASA: https://zulu.ssc.nasa.gov/mrsid/mrsid.pl

Digital Elevation Data free of Charge:

http://srtm.csi.cgiar.org/SELECTION/inputCoord.asp
http://glcfapp.glcf.umd.edu:8080/esdi/index.jsp
http://www.gdem.aster.ersdac.or.jp/search.jsp

ISSN 8755-6839

SCIENCE OF **TSUNAMI HAZARDS**

Journal of Tsunami Society International

Volume 30 **Number 3** **2011**

TSUNAMI SOCIETY INTERNATIONAL, 1741 Ala Moana Blvd. #70, Honolulu, HI 96815,USA.

WWW.TSUNAMISOCIETY.ORG